J. Fluid Mech. (1995), *vol.* 295, *pp.* 61–89

A series solution of the nonlinear wind-driven ocean circulation and its inertial limit

By W. T. M. VERKLEY[1]† AND J. T. F. ZIMMERMAN[1,2]

[1] Netherlands Institute for Sea Research, Den Burg (Texel), The Netherlands

[2] Institute of Marine and Atmospheric Sciences, University of Utrecht, The Netherlands

(Received 25 April 1994 and in revised form 10 April 1995)

A series solution approach to the forced and damped quasi-geostrophic barotropic vorticity equation is considered in order to examine the strongly forced and inertial limits of ocean gyre dynamics. The strongly forced limit is the limit investigated numerically by Veronis (1966*b*). It is shown that this limit, although superficially having the same symmetry properties as the inertial limit, is distinguishably different from the latter. After isolating the inertial limit in an appropriate way it is shown that our series solution method is able to find the 'free mode' and its 'almost free correction', that the 'free mode' obeys the integral criteria of Niiler (1966) and Pierrehumbert & Malguzzi (1984) and that the relationship between the streamfunction and the absolute vorticity is in general a nonlinear one.

1. Introduction

Wind-driven ocean circulation is a subject with a long history. Someone looking at the topics of present day theoretical research, like eddy-driven circulation, thermocline ventilation, vorticity homogenization and recirculation, all usually with a strong baroclinic component, will find these subjects rather remote from those of earlier days when, starting with Stommel's (1948) linear beta-plane model, the nonlinear barotropic quasi-geostrophic vorticity equation was the paradigm of gyre dynamics. One might think that all properties of that equation have been understood and/or that all unsolved problems are no longer of interest to present day theories. However, it is our feeling not only that there are indeed important unsolved aspects of the simplest model of nonlinear ocean circulation, but also that a solution of the outstanding problems can be of benefit when dealing with more sophisticated theories. This applies particularly to the question of the inertial limit of ocean gyre dynamics, which is the main theme of this paper.

In a sense nearly all properties of nonlinear barotropic wind-driven ocean circulation with bottom friction are contained in the sequence of numerical simulations by Veronis (1966*a*, *b*), repeated later on by Harrison & Stalos (1982). Principally this sequence shows the symmetry properties of a gyre for increasing forcing and constant friction. In the limit of weak forcing the Stommel solution is recovered with an east–west symmetry axis for symmetric forcing. The solution is characterized by a boundary layer current along the west side of the basin, which breaks the symmetry around the north–south axis. In the limit of strong forcing the symmetry axis runs more or less

† Present address and address for correspondence: Royal Netherlands Meteorological Institute, PO Box 201, 3730 AE De Bilt, The Netherlands.

north–south but the symmetry breaking due to the boundary layer current, which now runs along the north side of the basin, is weaker. In the intermediate regime all symmetry is lost but in a sense the 'symmetry'-axis is gradually turning in the direction of the circulation with increasing forcing. These symmetry properties of the nonlinear barotropic vorticity equation have recently been re-examined by Zimmerman & Maas (1989), Zimmerman (1993) and de Swart & Zimmerman (1993).

The fact that in the limit of strong forcing the circulation has a north–south symmetry axis has sometimes led to an interpretation of that limit as an inertial mode in the sense of Fofonoff (1954, 1962); see Veronis (1966*b*), Niiler (1966), Holloway (1986) and Pedlosky (1987, p. 315). This interpretation, however, has never been substantiated and it is the principal message of this paper to show that it cannot be substantiated because it is a false interpretation. As has been stressed by Zimmerman & Maas (1989) and Zimmerman (1993) any truly inertial circulation must have vanishingly small forcing and friction in order to be classified as such. Here we pursue the discussion in which our aims are the following. (i) To show simply, in essence by means of an absolute vorticity versus streamfunction scatter plot, that the limit of strong forcing is not an inertial limit. (ii) To define properly the inertial limit in ocean circulation theory and to show that in that limit a unique solution of the circulation obeying the integral criteria of Niiler (1966) and Pierrehumbert & Malguzzi (1984) can be obtained and finally (iii) to show that in general the inertial limit does not have a linear relationship between absolute vorticity and streamfunction as in the Fofonoff mode. We do so by employing the series solution method of Zimmerman (1993) that we modify in order to discuss the inertial limit. Our treatment resembles to a certain extent that of Merkine, Mo & Kalnay (1985), although our series expansion for the inertial mode is more direct and simpler. It furthermore provides all higher-order terms in a systematic way and as a consequence gives a direct proof of the generally nonlinear relationship between streamfunction and absolute vorticity.

The general outline is given in §2. The Veronis sequence and its limit of strong forcing is discussed in §3. The remaining two sections contain our primary results with respect to the inertial limit., In §4 we derive the series solutions for the 'free mode' and the 'almost free correction' stressing that of all possible solutions of the former only a single unique one is selected by a solvability criterion due to the latter – i.e. due to weak forcing and friction. Finally in §5 we show that the functional relationship between absolute vorticity and streamfunction of the free mode is in general a nonlinear one which asymptotically may become linear in a specific part of the parameter regime. In the Appendix we show that the terms in the series solution can be calculated exactly by a spectral method that allows a quick calculation of the series to any desired order. The convergence properties of the series are also discussed in the Appendix.

2. The wind-driven ocean circulation – two perturbation series

The system that is studied is the forced and damped barotropic vorticity equation on a beta-plane. Its steady-state form reads

$$\kappa\zeta + J(\psi, \zeta + y) + \tau = 0, \tag{1}$$

where $\zeta = \nabla^2\psi$. The operators ∇^2 and J are the Laplace and Jacobi operators for a flat surface, ζ is the relative vorticity, ψ the streamfunction and $f = y$ the Coriolis parameter. The system is forced by a field $-\tau$, the curl of the wind stress divided by the depth of the fluid, and damped by bottom friction $\kappa\zeta$. The system is non-

dimensionalized by measuring lengths in units of the lengthscale R (characteristic of the size of the basin) and time in units of $(\beta R)^{-1}$, where β is the northward derivative of the Coriolis parameter. This means that for the dimensional quantities, marked with asterisks, we have $\zeta_* = \zeta\beta R$, $\psi_* = \psi\beta R^3$, $\kappa_* = \kappa\beta R$ and $\tau_* = \tau\beta^2 R^2$. The non-dimensional number $\tau = \tau_*/(\beta^2 R^2)$ will be referred to as the Rossby number. It is the ratio of the Sverdrup velocity scale τ_*/β to the rotation velocity scale βR^2 and conforms in this sense to the usual definition of the Rossby number as given in Pedlosky (1987, p. 3). The non-dimensional number $\kappa = \kappa_*/\beta R$ will be referred to as the Ekman number. In the general sense that this number is the ratio of the frictional decay rate κ_* and the rotation rate βR, this definition also conforms to the definition of Pedlosky (1987, p. 191). Because we wish to exclude any influence from outside on the symmetry properties of (1), we assume that the forcing $-\tau$ is uniform in space. For the same reason we choose the ocean basin to be a circle with radius R. We will use Cartesian coordinates x and y as well as polar coordinates r and θ, where $x = r\cos\theta$ and $y = r\sin\theta$. In terms of these coordinates the Laplace and Jacobi operators read

$$\nabla^2\eta = \frac{\partial^2\eta}{\partial x^2} + \frac{\partial^2\eta}{\partial y^2} = \frac{1}{r}\frac{\partial}{\partial r}\left(r\frac{\partial\eta}{\partial r}\right) + \frac{1}{r^2}\frac{\partial^2\eta}{\partial\theta^2}, \tag{2}$$

$$J(\eta,\sigma) = \frac{\partial\eta}{\partial x}\frac{\partial\sigma}{\partial y} - \frac{\partial\eta}{\partial y}\frac{\partial\sigma}{\partial x} = \frac{1}{r}\left(\frac{\partial\eta}{\partial r}\frac{\partial\sigma}{\partial\theta} - \frac{\partial\eta}{\partial\theta}\frac{\partial\sigma}{\partial r}\right). \tag{3}$$

In terms of the Rossby number τ and the Ekman number κ we define two new parameters, which we will call δ and α, by

$$\delta \equiv \tau/(2\kappa), \tag{4}$$

$$\alpha \equiv \tau/(2\kappa^2) = \delta/\kappa, \tag{5}$$

which, expressed in dimensional quantities, are $\delta = \tau_*/2\beta R\kappa_*$ and $\alpha = \tau_*/2\kappa_*^2$. The number δ, being half of the non-dimensional ratio of the forcing and friction parameters, can be interpreted as a measure of the strength (in terms of vorticity) of the circulation. The number α relates this strength to the friction parameter and can therefore be interpreted as a measure of nonlinearity. For this reason α is sometimes called the Reynolds number. We note that β is absent in the dimensional expression for α. This allows us to study the effect of increasing nonlinearity (increasing α) for small values of β. This leads naturally to the idea of expanding (1) in terms of a power series in β. This is effectively what we do if we expand (1) in a power series of κ^{-1} or δ^{-1}, as can be seen from the dimensional expressions for κ and δ. An expansion in κ^{-1} turns out to be convenient in studying the Veronis sequence and will be applied in §3. An expansion in δ^{-1} is appropriate in studying an alternative sequence and the inertial limit which are the subjects of §§4 and 5. We now give these two perturbation expansions, starting with the expansion in κ^{-1} and continuing with the expansion in δ^{-1}.

2.1. *A perturbation series in* κ^{-1}

Expressing τ in terms of α and dividing (1) by κ allows us to write this equation as

$$\zeta + \kappa^{-1}J(\psi, \zeta + y) + 2\kappa\alpha = 0. \tag{6}$$

Following Zimmerman (1993) we expand ζ and ψ in terms of a power series in κ^{-1}, i.e. we write

$$\zeta = \kappa\zeta_{-1} + \zeta_0 + \kappa^{-1}\zeta_1 + \kappa^{-2}\zeta_2 + \ldots, \tag{7a}$$

$$\psi = \kappa\psi_{-1} + \psi_0 + \kappa^{-1}\psi_1 + \kappa^{-2}\psi_2 + \ldots. \tag{7b}$$

Substituting these expansions into (6) and collecting like powers of κ^{-1}, we obtain a hierarchy of equations. At order -1 we have

$$\zeta_{-1}+J(\psi_{-1},\zeta_{-1})=-2\alpha, \tag{8}$$

the solution of which reads:

$$\zeta_{-1}=-2\alpha, \quad \psi_{-1}=-\tfrac{1}{2}\alpha(r^2-1). \tag{9a, b}$$

Owing to the solution (9) for ζ_{-1} and ψ_{-1} we have

$$J(\psi_{-1},\eta)=-\alpha\frac{\partial\eta}{\partial\theta}, \quad J(\eta,\zeta_{-1})=0, \tag{10a, b}$$

for any field η. Using (10), the hierarchy of equations can then be written as

$$\zeta_{-1}=-2\alpha, \tag{11a}$$

$$(1-\alpha\partial/\partial\theta)\zeta_0=\alpha x, \tag{11b}$$

$$(1-\alpha\partial/\partial\theta)\zeta_1=-J(\psi_0,\zeta_0+y), \tag{11c}$$

$$(1-\alpha\partial/\partial\theta)\zeta_2=-J(\psi_0,\zeta_1)-J(\psi_1,\zeta_0+y), \tag{11d}$$

$$\vdots$$

$$(1-\alpha\partial/\partial\theta)\zeta_k=-J(\psi_0,\zeta_{k-1})-J(\psi_1,\zeta_{k-2})-\ldots-J(\psi_{k-1},\zeta_0+y),$$

$$\vdots$$

Equations (7) and (11) are the basic perturbation series in κ^{-1}.

2.2. *A perturbation series in* δ^{-1}

Dividing (1) by $\alpha\kappa$ and using the definitions (4) and (5) of δ and α, we obtain the following alternative form of (1):

$$\alpha^{-1}\zeta+\delta^{-1}J(\psi,\zeta+y)+2\delta\alpha^{-1}=0. \tag{12}$$

Because δ is proportional to κ, we might indeed expand ζ and ψ in a power series in δ^{-1}, i.e.

$$\zeta=\delta\xi_{-1}+\xi_0+\delta^{-1}\xi_1+\delta^{-2}\xi_2+\ldots, \tag{13a}$$

$$\psi=\delta\chi_{-1}+\chi_0+\delta^{-1}\chi_1+\delta^{-2}\chi_2+\ldots. \tag{13b}$$

In a similar way as we derived (11) from (6) the equations for the different orders in δ^{-1} are obtained as

$$\xi_{-1}=-2, \tag{14a}$$

$$(\alpha^{-1}-\partial/\partial\theta)\xi_0=x, \tag{14b}$$

$$(\alpha^{-1}-\partial/\partial\theta)\xi_1=-J(\chi_0,\xi_0+y), \tag{14c}$$

$$(\alpha^{-1}-\partial/\partial\theta)\xi_2=-J(\chi_0,\xi_1)-J(\chi_1,\xi_0+y), \tag{14d}$$

$$\vdots$$

$$(\alpha^{-1}-\partial/\partial\theta)\xi_k=-J(\chi_0,\xi_{k-1})-J(\chi_1,\xi_{k-2})-\ldots-J(\chi_{k-1},\xi_0+y).$$

$$\vdots$$

Equations (13) and (14) are the basic perturbation series in δ^{-1}. By comparing (11) with (14) it can be seen that there is a simple relation between the fields ζ_k and ξ_k and between ψ_k and χ_k, namely,

$$\xi_k = \alpha^k \zeta_k, \quad \chi_k = \alpha^k \psi_k. \tag{15a, b}$$

The solutions at different order in these expansions still depend parametrically on α. Thus, looking particularly at the strongly nonlinear regime of each of these solutions – as a series in κ^{-1} or in δ^{-1} – each can be expanded subsequently in α^{-1}. In the next sections we shall show that the final asymptotic result has a quite different physical interpretation for the series in κ^{-1} to that in δ^{-1}.

2.3 *Solving the equations*

Equations (11) and (14) can be solved consecutively. To give an impression of the type of solutions to be expected from these series we consider (11*b*) and (11*c*). Equation (11*b*) is solved by

$$\zeta_0 = \frac{\alpha}{(1+\alpha^2)}(r\cos\theta - \alpha r \sin\theta), \tag{16a}$$

$$\psi_0 = \frac{\alpha}{8(1+\alpha^2)}(r^2-1)(r\cos\theta - \alpha r\sin\theta). \tag{16b}$$

For the Jacobian of ψ_0 and $\zeta_0 + y$ we then have

$$J(\psi_0, \zeta_0 + y) = \frac{\alpha}{8(1+\alpha^2)^2}[(1+\alpha^2)(2r^2-1) + (1-\alpha^2)r^2\cos 2\theta - 2\alpha r^2 \sin 2\theta]. \tag{17}$$

This means that the solution of (11*c*) is given by

$$\zeta_1 = -\frac{\alpha}{8(1+\alpha^2)^2} \times \left[(1+\alpha^2)(2r^2-1) + \frac{(1-5\alpha^2)}{(1+4\alpha^2)} r^2\cos 2\theta - \frac{\alpha(4\alpha - 2\alpha^2)}{(1+4\alpha^2)} r^2 \sin 2\theta\right], \tag{18a}$$

$$\psi_1 = -\frac{\alpha}{8(1+\alpha^2)^2}\frac{(r^2-1)}{4} \times \left[\frac{(1+\alpha^2)}{2}(r^2-1) + \frac{(1-5\alpha^2)}{3(1+4\alpha^2)} r^2\cos 2\theta - \frac{\alpha(4\alpha-2\alpha^2)}{3(1+4\alpha^2)} r^2 \sin 2\theta\right]. \tag{18b}$$

The fact that the Laplacian of the given streamfunctions leads to the given relative vorticity fields can be checked by using (2). Note that ξ_0 and χ_0 in the corresponding expansion in δ^{-1} are identical to ζ_0 and ψ_0. The fields of order 1 in the δ^{-1} expansion are α times the fields in the κ^{-1} expansion. Apart from the monopole term in the first-order solution, these expressions are identical to those of Zimmerman (1993).

In the Appendix we show how solutions can be obtained to any desired order using a spectral method. In this method the fields are represented in terms of the functions $X_{mn}(r,\theta) \equiv r^n e^{im\theta}$, where $m = \ldots -2, -1, 0, 1, 2, \ldots$, and $n = |m| + 2p$ with $p = 0, 1, 2, \ldots$. If $-N \leqslant m \leqslant N$ and $n \leqslant N$ these functions span the same linear vector space as $1, x, y, x^2, xy, y^2, \ldots, x^N, x^{N-1}y, \ldots, xy^{N-1}, y^N$, which space will be denoted by TN. In the Appendix it is shown how the different operators appearing in (11) and (14)

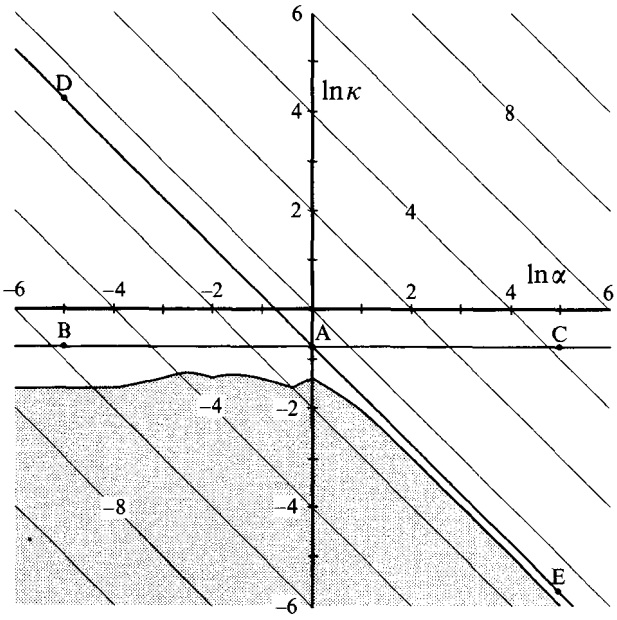

FIGURE 1. The parameter space of the model, with $\ln\alpha$ on the horizontal axis and $\ln\kappa$ on the vertical axis. The sloping thin solid lines are isolines of δ. Points above the thick solid curve correspond to α, κ and δ values for which the series expansion converges uniformly over the whole basin. Beneath this curve the convergence is not uniform and for clarity this region has been shaded. The solid horizontal line denotes the Veronis sequence, discussed in §3, with B, A and C as representative examples. The solid sloping line denotes the sequence to the inertial limit, with examples D, A and E, which is discussed in §§4 and 5.

can be represented. It is also shown that fields ζ_k and ψ_k that result from solving the kth equation (11) (and the fields ξ_k and χ_k in (14)) have the following properties. First, ζ_k is an element of $T(k+1)$ and ψ_k is an element of $T(k+3)$ with $|m| \leqslant k+1$. Secondly, for even k the fields ζ_k and ψ_k are expressed in functions X_{mn} with odd m, and for odd k the fields ζ_k and ψ_k only contain functions X_{mn} with even m.

In the Appendix there is an investigation of the conditions under which the series expansions converge. The result is given in figure 1. The abscissa is $\ln\alpha$ and the ordinate is $\ln\kappa$. The thin sloping straight lines denote values of constant δ. Points above the solid curve correspond to parameters α, κ and δ for which the series expansions for ζ converge uniformly. Points beneath the curve correspond to parameters for which the series expansions do not converge uniformly, although the series might converge locally. For clarity the region beneath the curve has been shaded. The Veronis sequence is a series of solutions for which κ is constant. An example of such a sequence is marked in figure 1 by the solid horizontal line. This sequence, and in particular the solutions A, B and C, will be discussed in the next section, using the series expansion in κ^{-1}. Figure 1 shows, however, that the expansions also allow us to consider a sequence in which δ is kept fixed as long as its value is large enough. Such an alternative sequence is marked by the sloping solid line in figure 1. This sequence and its representative points A, D and E will be discussed in §§4 and 5, using the series expansion in δ^{-1}.

			Figure 2		
-9.67×10^{-1}	9.55×10^{-1}	-1.75	-3.35×10^{-1}	-1.40219×10^{2}	-1.40205×10^{2}
-1.63×10^{-2}	-2.48×10^{-3}	-1.78	-4.07×10^{-1}	-1.41174×10^{2}	-1.39251×10^{2}
1.32×10^{-5}	1.49×10^{-3}	1.98×10^{-3}	2.28×10^{-1}	4.47452×10^{-1}	3.50525×10^{1}
			Figure 3		
-2.83	-8.53×10^{-1}	-2.41	-3.67×10^{-1}	-2.33	-1.44×10^{-1}
3.84×10^{-3}	3.80×10^{-1}	1.96×10^{-3}	2.21×10^{-1}	9.09×10^{-4}	1.23×10^{-1}
			Figure 4		
-1.91	1.68×10^{-2}	-1.75	-3.35×10^{-1}	-1.20	-7.04×10^{-1}
-9.51×10^{-1}	-9.38×10^{-1}	-1.78	-4.07×10^{-1}	-2.15	-2.17×10^{-1}
3.01×10^{-3}	2.36×10^{-1}	1.98×10^{-3}	2.28×10^{-1}	1.90×10^{-3}	2.21×10^{-1}
			Figure 5(a)		
-2.66	-2.47	-1.71	-1.40	-1.20	-7.04×10^{-1}
-3.62	-1.69	-2.67	-7.38×10^{-1}	-2.14	-2.17×10^{-1}
7.01×10^{-3}	6.36×10^{-1}	3.81×10^{-3}	3.80×10^{-1}	1.90×10^{-3}	2.21×10^{-1}
			Figure 5(b)		
-9.88×10^{-1}	9.88×10^{-1}	-1.01	1.01	-1.06	1.06
-4.70×10^{-2}	4.70×10^{-2}	-4.54×10^{-2}	4.54×10^{-2}	-4.17×10^{-2}	4.17×10^{-2}
			Figure 9		
-1.27	1.27	-1.46	-2.33×10^{-2}	-1.42	-7.57×10^{-3}
-1.27	1.27	-1.54	-8.37×10^{-2}	-1.47	-1.34×10^{-1}
7.14×10^{-4}	1.55×10^{-1}	7.39×10^{-4}	1.32×10^{-1}	8.96×10^{-4}	1.31×10^{-1}

TABLE 1. Minimum and maximum values, of the fields shown in figures 2, 3, 4, 5(a, b) and 9. The maximum values in the fields occur around the position marked by H in the figures. The first pair of two columns gives the minima and maxima of the fields in the first column of the figures, the second pair of columns gives the minima and maxima of the fields in the second column of the figures, etc. The contour interval is always $\frac{1}{8}$ times the difference between minima and maxima. The extreme values were obtained from a 51×51 grid $x_{ij}=-1+(i-1)/25$, $y_{ij}=-1+(j-1)/25$ with $x_{ij}^2+y_{ij}^2<1$.

3. The Veronis sequence

As mentioned in the Introduction, the basic symmetry properties of the quasi-geostrophic vorticity equation (1) have been discovered by Veronis (1966*b*) in a series of numerical simulations. Essentially this series is one of increasing forcing (Rossby number) keeping the damping (Ekman number) fixed. In terms of the parameters α and κ, this sequence corresponds to a horizontal line in figure 1. If we identify the radius R of our basin with half of the width of Veronis' square basin $(\pi/2)L$, then the sequence that Veronis studied can be described as one in which the values of $(\ln\alpha, \ln\kappa)$ are $(-8.52, -3.45)$, $(-1.71, -3.45)$, $(-0.69, -3.45)$, $(0.69, -5.51)$, $(2.08, -4.14)$, $(2.74, -4.74)$ and $(3.47, -4.14)$. The first of these cases corresponds with Veronis' figure 4, the last one with his figure 9 (lower). Note that the last case falls within the region in which our series expansion converges. The particular sequence that we will investigate is denoted by the horizontal line drawn in figure 1. The points B, A and C are typical members of this sequence, corresponding to $(\ln\alpha, \ln\kappa) = (-5.00, -0.75)$, $(0, -0.75)$ and $(5.00, -0.75)$. In figure 2 we show the associated absolute vorticity, relative vorticity, streamfunction and a scatter plot of absolute vorticity versus streamfunction of these solutions, calculated with the method described in §2.1 and the Appendix, summing terms up to $k = 50$. The plots in figure 2 summarize the basic features of the Veronis sequence. First, we see that for both small and large values of α the relative vorticity and the streamfunction of the solution are symmetric; for small values of α around an east–west axis, for large values of α around a north–south

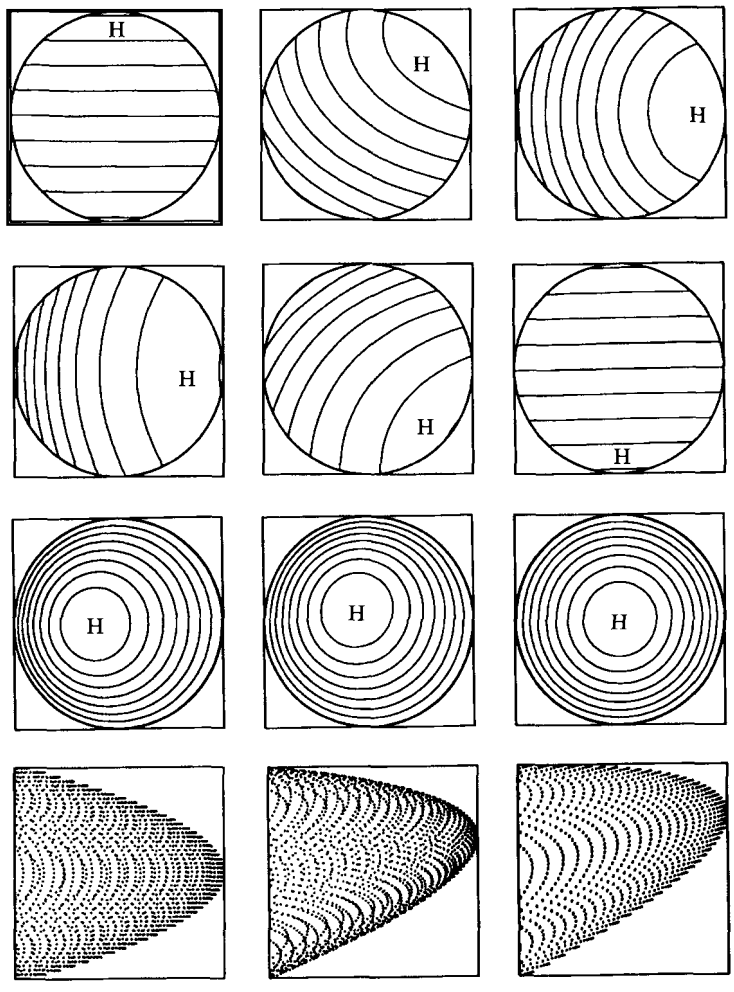

FIGURE 2. The absolute vorticity (first row), relative vorticity (second row), streamfunction (third row) and scatter diagram (fourth row) of absolute vorticity against streamfunction of the solutions corresponding to the points B, A and C of the Veronis sequence, depicted graphically by the solid horizontal line in figure 1. The first column of plots correspond to point B, the second to point A and the third to point C in figure 1. The fields were calculated by summing the terms of the series expansion in κ^{-1} up to $k = 50$. The extreme values in this figure and in figures 2, 3, 4, 5(a, b) and 9 are given in table 1. High values of the plotted fields occur around the symbol H.

axis albeit with a lesser displacement of the circulation centre with respect to the basin centre than in the small α case. (In the large-α case the displacement of the circulation centre is so small as to be not noticeable in the streamfunction plot.) Going from small to large values of α, the symmetry axis turns from east–west to north–south although, in fact, the symmetry is broken at intermediate values of α. Indeed, in this case – exemplified by point A in figure 1 and the second column of plots in figure 2 – all symmetry is lost, which is most clear in the relative vorticity field. The influence of the latter on the absolute vorticity field is evident in the strong northward bending of the contour lines on the north-western side of the basin. All these features are recovered in the analytic expressions up to order 1 as given in (9), (16) and (18). This was the main point in the work of Zimmerman (1993).

In the Veronis sequence two limiting cases are of special interest. The first is the limit in which $\alpha \to 0$ ($\ln \alpha \to -\infty$). Since $\alpha = \tau/2\kappa^2$, this is the limit in which the forcing becomes very much smaller than the friction. As the amplitude of the solution will be very small, the system is essentially linear and the corresponding limit might be called the linear limit. This limit will be discussed in §3.1. The other limit is $\alpha \to \infty$ ($\ln \alpha \to \infty$). This is the limit of strong forcing, discussed in §3.2. Subsection 3.1 mainly serves to illustrate the series expansion in κ^{-1} in a case in which the exact solution is known. Readers who are not particularly interested in the linear limit *per se* may skip §3.1 and continue with §3.2, without losing the thread of the argument.

3.1. *The limit of weak forcing – the linear limit*

In the linear limit α becomes vanishingly small while κ is kept constant. In view of definition (5), this means that the forcing $\tau = 2\alpha\kappa^2$ becomes vanishingly small. We may analyse the system in the usual way by choosing a particular value of κ and expand ζ and ψ in power series in α:

$$\zeta = \zeta^0 + \alpha\zeta^1 + \alpha^2\zeta^2 + \ldots, \quad \psi = \psi^0 + \alpha\psi^1 + \alpha^2\psi^2 + \ldots. \tag{19a, b}$$

Note that on α the superscripts denote powers, whereas on ζ and ψ they denote orders. Multiplying (6) with κ and substituting (19) for ζ and ψ, we find that $\zeta^0 = 0$ and $\psi^0 = 0$ and that ζ^1 and ψ^1 satisfy the linear Stommel equation (Stommel 1948):

$$\kappa\zeta^1 + \frac{\partial\psi^1}{\partial x} + 2\kappa^2 = 0. \tag{20}$$

The exact solution for a circular basin reads, in terms of the streamfunction (Beardsley 1969),

$$\psi^1 = -2\kappa^2\left[r\cos\theta - \mathrm{e}^{(-r\cos\theta/(2\kappa))}\left\{\frac{I_1(1/(2\kappa))\, I_0(r/(2\kappa))}{I_0(1/(2\kappa))} + \sum_{m=1}^{\infty}\cos m\theta\left(\frac{I_{m+1}(1/(2\kappa)) + I_{m-1}(1/(2\kappa))}{I_m(1/(2\kappa))}\right) I_m(r/(2\kappa))\right\}\right], \tag{21}$$

where I_m is the mth order-modified Bessel function of the first kind.

The purpose of the rest of this subsection is to show that if we apply the expansion in α to each of the equations in the hierarchy (11) and retain only the zeroth- and first-order terms, one naturally arrives at a solution of the Stommel equation. For the fields ζ_k and ψ_k in (11) we write

$$\zeta_k = \zeta_k^0 + \alpha\zeta_k^1 + \alpha^2\zeta_k^2 + \ldots, \quad \psi_k = \psi_k^0 + \alpha\psi_k^1 + \alpha^2\psi_k^2 + \ldots, \tag{22a, b}$$

which gives the following expressions for ζ^l and ψ^l ($l = 0, 1, 2, \ldots$) in (19):

$$\zeta^l = \kappa\zeta_{-1}^l + \zeta_0^l + \kappa^{-1}\zeta_1^l + \ldots, \quad \psi^l = \kappa\psi_{-1}^l + \psi_0^l + \kappa^{-1}\psi_1^l + \ldots. \tag{23a, b}$$

It can then be shown that all terms $\zeta_k^0 (k = -1, 0, 1, \ldots)$ are zero and that

$$\zeta_{-1}^1 = -2, \quad \zeta_k^1 = -J(\psi_{k-1}^1, y) = -\frac{\partial\psi_{k-1}^1}{\partial x}, \tag{24a, b}$$

the latter expression applying for $k \geqslant 0$. The corresponding streamfunctions can be obtained by using the expressions in §A 1 of the Appendix. We see that ζ^0 (and therefore ψ^0), as given by (23), is identically zero as it should. By substituting (24) in (23a) we can check that our series expansion for ζ^1 is a solution of the Stommel

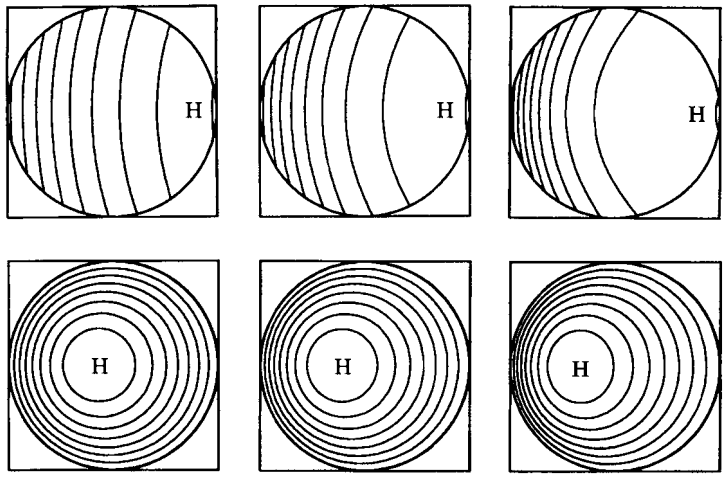

FIGURE 3. The relative vorticity ζ^1 (first row) and the streamfunction ψ^1 (second row) of the solution in the linear limit, calculated using the series expansion in κ^{-1} up to $k = 50$. In the first column the value of $\ln\kappa$ is -0.25, in the second column the value of $\ln\kappa$ is -0.75 and in the last column $\ln\kappa$ is -1.25. The fields in the middle column should be compared with those of the first column in figure 2, where the solution is shown for the same value of κ but with a small though non-vanishing value of α.

equation (20). Using the method described in §A 3 of the Appendix we find that the series expansion for ζ^1 converges uniformly if $\ln\kappa > -1.57$. As an illustration, we calculated three examples of ζ^1 and ψ^1, summing terms up to $k = 50$. The results, for $\ln\kappa = -0.25$, -0.75 and -1.25, are shown in figure 3. The middle case should be compared with the first column of figure 2, which shows the solution for the same value of κ but with a small though non-zero value of α.

Expressions (24) allow us to calculate a few low-order terms of ζ^1 and ψ^1. For the relative vorticity ζ^1 we have

$$\zeta^1_{-1} = -2, \quad \zeta^1_0 = r\cos\theta, \quad \zeta^1_1 = -\tfrac{1}{8}[2r^2 - 1 + r^2\cos 2\theta], \tag{25a–c}$$

and for the streamfunctions ψ^1

$$\psi^1_{-1} = -\tfrac{1}{2}(r^2-1), \quad \psi^1_0 = \tfrac{1}{8}(r^2-1)r\cos\theta, \tag{26a,b}$$

$$\psi^1_1 = -\tfrac{1}{32}(r^2-1)[\tfrac{1}{2}(r^2-1) + \tfrac{1}{3}r^2\cos 2\theta]. \tag{26c}$$

It can be checked that these results are in accordance with the general expressions (9), (16) and (18) by taking the limit for vanishingly small α and keeping terms of order α. It can also be verified that the results comply with the general solution (21) of the Stommel equation by expanding (21) in κ^{-1}. All relevant properties of the linear limit as displayed in figure 3 can easily be deduced from these low-order expressions, in particular the strictly western intensification (only $\cos m\theta$-terms in the expansion) and the equality of absolute and planetary vorticity.

3.2. *The limit of strong forcing*

In the limit in which the number α goes to infinity, keeping the value of the Ekman number κ fixed we encounter a strongly nonlinear regime characterized by strong forcing. We can analyse this regime by writing ζ_k and ψ_k of the hierarchy (11) in a power series in α^{-1}, starting with α. From (9) it follows that such a series for ζ_{-1} and ψ_{-1} consists of only one term proportional to α. By dividing (11*b*) by α, it follows that the expansion of ζ_0 (and thus of ψ_0) starts with a term independent of α followed by

terms of order α^{-1}, α^{-2}, etc. In the same way it can be seen that the expansions of ζ_1 and ψ_1 start with α^{-1}, that the expansions of ζ_2 and ψ_2 start with α^{-2}, etc. So, if we are only interested in the total solution up to order α^{-1}, we can limit ourselves to $k = -1$, 0 and 1 in the κ^{-1} expansion. As the exact results for these terms are given in §2, we can expand these expressions in a power series in α^{-1} to find that

$$\zeta = -2\alpha\kappa - r\sin\theta - \frac{1}{\alpha} r\cos\theta - \frac{1}{8\alpha\kappa}(2r^2-1) + O(\alpha^{-2}), \tag{27}$$

$$\psi = -\tfrac{1}{2}\alpha\kappa(r^2-1) - \tfrac{1}{8}(r^2-1)\, r\sin\theta + \frac{1}{8\alpha}(r^2-1)\, r\cos\theta - \frac{1}{64\alpha\kappa}(r^2-1)^2 + O(\alpha^{-2}), \tag{28}$$

$$\zeta + y = -2\alpha\kappa - \frac{1}{\alpha} r\cos\theta - \frac{1}{8\alpha\kappa}(2r^2-1) + O(\alpha^{-2}). \tag{29}$$

For the discussion of the inertial limit in the next sections the following properties of this solution are of importance. First we note that in the limit of strong forcing the dominant term of the streamfunction is a circularly symmetric monopole with a constant relative vorticity as if the beta-effect were absent. At the next order (α^0) a weak dipole still exists which breaks the symmetry of the total streamfunction around the east–west axis. The relative vorticity at this order in α is a linear function of the north–south coordinate and exactly annihilates the planetary vorticity gradient. Thus at order α^0 the absolute vorticity vanishes. In consequence, the breaking of the circular symmetry of the absolute vorticity appears for the first time at the next order (α^{-1}). Quite evidently then, in this strongly forced nonlinear limit there is no unique relationship between absolute vorticity and streamfunction as can also be seen in the scatterplot for this limit in figure 2 (third column). This already is an indication that the regime where α goes to infinity keeping κ constant cannot be classified as an inertial regime. The proper definition of the latter is the subject of the next two sections.

4. The sequence to the inertial limit

In this section we will discuss a sequence of solutions in which α is varied from small to high values but in which now δ, i.e. the ratio between forcing and friction, is fixed. The sequence is represented graphically by the sloping solid line in figure 1. The points D, A and E are representative members of such a sequence, corresponding to $(\ln\alpha, \ln\delta) = (-5.00, -0.75), (0, -0.75)$ and $(5.00, -0.75)$. In figure 4 we show the associated absolute vorticity, relative vorticity, streamfunction and scatter diagrams of absolute vorticity versus streamfunction of these solutions, calculated with the method described in §2.2 and the Appendix, summing terms up to $k = 50$. We see that for both small and large values of α the relative vorticity and the streamfunction of the solution are symmetric: for small values of α around the east–west axis, for large values of α around the north–south axis. Going from small to large values of α, the symmetry axis turns towards a north–south direction although, again, the symmetry is broken at intermediate values of α. As far as the symmetry properties are concerned, this sequence is not unlike the Veronis sequence discussed in the previous section, but it should be stressed here that the present sequence has a quite different physical interpretation.

As in the Veronis sequence two limiting cases are of special interest. The first is the limit in which $\alpha \to 0$ ($\ln\alpha \to -\infty$). Since $\alpha = \delta/\kappa$ and δ is kept constant, this is the limit in which both the forcing and the friction become very large. This limit will be

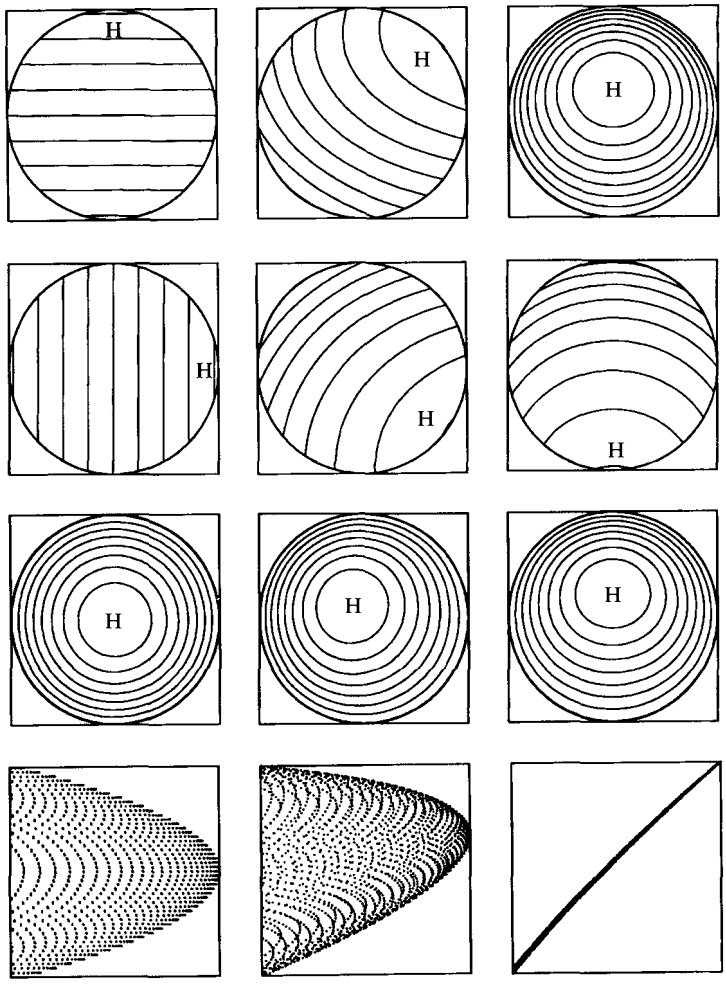

FIGURE 4. The absolute vorticity (first row), relative vorticity (second row), streamfunction (third row) and scatter diagram (fourth row) of absolute vorticity against streamfunction of the solutions corresponding to the points D, A and E of the sequence to the inertial limit, depicted graphically by the sloping solid line in figure 1. The first column of plots correspond to point D, the second to point A and the third to point E in figure 1. The fields were calculated by summing the terms of the series expansion in δ^{-1} up to $k = 50$.

discussed in §4.1. The other limit is the case in which $\alpha \to \infty$ ($\ln \alpha \to \infty$). In this limit both the forcing and the friction become vanishingly small. This limit is the inertial limit and will be discussed in §§4.2 and 5.

4.1. *The limit of strong forcing and friction*

In the limit in which α goes to zero, keeping the value of δ fixed we encounter a regime characterized by strong forcing and friction. The fact that α approaches zero in this limit suggests that we expand the different terms ξ_k and χ_k in (13) in a power series in α. We see from (14) that such an expansion of ξ_{-1} and χ_{-1} has only one term, and this term is independent of α. By multiplying (14*b*) with α it can be seen that the expansion of ξ_0 and χ_0 starts with a term proportional to α. From (14*c*) it follows that the expansion of ξ_1 and χ_1 starts with a term proportional to α^2, etc. So, in analogy with the limit of strong forcing in the Veronis sequence, we only need to consider the -1,

0 and 1 order terms in the δ^{-1} expansion if we are satisfied with the solution up to order α^2. Again, we can then take the analytic expressions given in §2.3 and expand them in a power series in α to find that we have in the limit of strong forcing and friction

$$\zeta = -2\delta + \alpha r\cos\theta - \alpha^2 r\sin\theta - \frac{\alpha^2}{8\delta}(2r^2 - 1 + r^2\cos 2\theta) + O(\alpha^3), \tag{30a}$$

$$\psi = -\tfrac{1}{2}\delta(r^2-1) + \tfrac{1}{8}\alpha(r^2-1)\,r\cos\theta - \tfrac{1}{8}\alpha^2(r^2-1)\,r\sin\theta - \frac{\alpha^2}{64\delta}(r^2-1)\,(r^2 - 1 + \tfrac{2}{3}r^2\cos 2\theta) + O(\alpha^3), \tag{30b}$$

$$\zeta + y = -2\delta + r\sin\theta + \alpha r\cos\theta - \alpha^2 r\sin\theta - \frac{\alpha^2}{8\delta}(2r^2 - 1 + r^2\cos 2\theta) + O(\alpha^3). \tag{30c}$$

The expression for the streamfunction shows that the circulation is nearly circularly symmetric. The relative vorticity field is, to first order in α, a linear function of the west–east coordinate. So the symmetry of the solution is weakly broken along the north–south axis and therefore basically of the 'Stommel' type, i.e. basically of the form of the linear limit in the Veronis sequence.

4.2. *The limit of weak forcing and friction – the inertial limit*

More interesting, however, is the limit $\alpha = \tau/2\kappa^2 \to \infty$ with $\delta = \alpha\kappa = \tau/2\kappa$ kept constant. Note that now we have a strongly nonlinear limit with weak (asymptotically vanishing) forcing (τ) and friction (κ) as $\alpha \to \infty$, and $\tau/2\kappa$ is constant can only be realized by having $\kappa \to 0$, whence also $\tau \to 0$ in order to have $\tau/2\kappa$ constant. It has been argued before by Zimmerman & Maas (1989) and Zimmerman (1993) that this limit is the proper definition of an inertial mode in the forced and damped quasi-geostrophic vorticity equation. For here the nonlinear advection of absolute vorticity becomes the dominant term in the equation while forcing and damping, though constant in their ratio, become vanishingly small. Yet the circulation that is ultimately established is a result of the subtle balance between the weak effects of forcing and damping. In this subsection and in §5 we shall show that our series solution is able to solve the inherent degeneracy problem of any inertial circulation and of the related problem of the functional relationship between absolute vorticity and streamfunction.

Before discussing our series solution we first summarize the problems which one encounters in the traditional approach to the inertial limit. Because α goes to infinity in the inertial limit, it is natural to expand ζ and ψ in a power series in α^{-1}:

$$\zeta = \xi^0 + \alpha^{-1}\xi^1 + \alpha^{-2}\xi^2 + \ldots, \quad \psi = \chi^0 + \alpha^{-1}\chi^1 + \alpha^{-2}\chi^2 + \ldots. \tag{31a, b}$$

Note, again, that on α the superscripts denote powers, whereas on ξ and χ they denote orders. Equation (12) reads, after multiplying by δ,

$$\delta\alpha^{-1}\zeta + J(\psi, \zeta + y) + 2\delta^2\alpha^{-1} = 0. \tag{32}$$

Substituting in (32) the series expansions above and collecting like powers of α^{-1}, we get for the order 0 and 1 equations respectively:

$$J(\chi^0, \xi^0 + y) = 0, \quad \delta(\xi^0 + 2\delta) + J(\chi^0, \xi^1) + J(\chi^1, \xi^0 + y) = 0. \tag{33a, b}$$

These two equations contain the essence of the inertial circulation problem of the quasi-geostrophic vorticity equation. The first one (33*a*) describes the 'free mode', the second one what we shall call here the 'almost free correction'. Note that (33*b*) couples both modes. The first equation, (33*a*), expresses to zeroth order in α^{-1} the conservation

of absolute vorticity along a streamline of the zeroth-order field. This presents a degeneracy problem in that each absolute vorticity field that is a sufficiently smooth function of the streamfunction, i.e. that satisfies

$$\xi^0 + y = F(\chi^0), \tag{34}$$

is a solution of (33*a*). One way to circumvent the degeneracy problem is simply to postulate a functional relationship between $\xi^0 + y$ and χ^0 for which usually a linear one is chosen like in the classical solutions of Fofonoff (1954, 1962). If this linear function is written as $F(z) = a + bz$, it can be shown that the solution for a circular ocean basin is

$$\chi^0 = \frac{1}{b}\left[\left(\frac{I_0(b^{1/2}r)}{I_0(b^{1/2})} - 1\right)a + \left(r - \frac{I_1(b^{1/2}r)}{I_1(b^{1/2})}\right)\sin\theta\right], \tag{35}$$

where, as in the exact solution of the Stommel equation, I_m is an mth-order modified Bessel function of the first kind. That (35) indeed leads to the postulated linear relation between $\xi^0 + y$ and χ^0 can be verified by using that the functions $I_m(b^{1/2}r)\exp(im\theta)$ are eigenfunctions of the Laplace operator (2) with eigenvalue b.

We shall discuss the relationship between absolute vorticity and streamfunction in detail in the next section. Here we note that evidently the kind of inertial circulation that is established, and thus the functional form of the relationship between absolute vorticity and streamfunction, is ultimately set by the equation at first order in α^{-1}, i.e. by (33*b*) and thus by forcing and friction no matter how weak these are. Therefore (33*b*) must in principle be able to remove the degeneracy of (33*a*). Indeed, if one multiplies (33*b*) by an arbitrary function $G(\chi^0)$ and integrates the equation over the whole flow domain it follows that

$$\int_D G(\chi^0)(\xi^0 + 2\delta)\,\mathrm{d}S = 0. \tag{36}$$

Here D denotes the circular ocean basin and $\mathrm{d}S$ is an area element. If one now substitutes for $G(\chi^0)$ a function that is non-zero only in a vanishingly small range $\mathrm{d}\chi^0$ around a value $\chi^0 = c$, then this equation leads to

$$\oint_{\chi^0=c} (\xi^0 + 2\delta)\frac{\mathrm{d}l}{u^0} = 0, \tag{37}$$

where $\mathrm{d}l$ is a line element in a contour integral over the streamline $\chi^0 = c$ and u^0 is the velocity associated with χ^0. The condition above expresses that, in a time-averaged sense, the forcing and friction terms should balance over each streamline of the inertial flow χ^0. Evidently this is in fact a solvability condition to (33*a*) as the fields $\xi^0 + y$ and χ^0 have to satisfy (37) in order that they are consistent with (33*b*). In the present context, this integral relationship has first been formulated by Niiler (1966) and was later elaborated by Pierrehumbert & Malguzzi (1984). It was also used by Marshall & Nurser (1986) and by Greatbatch (1987) in the context of more general density-stratified systems. We will show that our series method leads to a unique solution of (33*a*) by explicitly constructing a solution of (33*b*).

To this end we return to the series expansion (13). We expand each of the fields ξ_k and $\chi_k (k = -1, 0, 1, 2, \ldots)$ in terms of a power series in α^{-1}:

$$\xi_k = \xi_k^0 + \alpha^{-1}\xi_k^1 + \alpha^{-2}\xi_k^2 + \ldots, \quad \chi_k = \chi_k^0 + \alpha^{-1}\chi_k^1 + \alpha^{-2}\chi_k^2 + \ldots, \tag{38a, b}$$

which gives for the fields ξ^l and $\chi^l (l = 0, 1, 2, \ldots)$ in (31) the following expressions:

$$\xi^l = \delta\xi_{-1}^l + \xi_0^l + \delta^{-1}\xi_1^l + \ldots, \quad \chi^l = \delta\chi_{-1}^l + \chi_0^l + \delta^{-1}\chi_1^l + \ldots. \tag{39a, b}$$

Then we substitute the expansions (38) in (14) and consider the terms up to the first order in α^{-1}.

Concerning (14*a*), the result of the procedure described above is immediately evident. Substituting the expansion for ξ_{-1} in (14*a*), we obtain

$$\xi^0_{-1} = -2, \quad \xi^1_{-1} = 0, \tag{40a, b}$$

and for the accompanying streamfunctions

$$\chi^0_{-1} = -\tfrac{1}{2}(r^2-1), \quad \chi^1_{-1} = 0, \tag{41a, b}$$

all higher-order terms, i.e. ξ^2_{-1}, ξ^3_{-1}, ... and χ^2_{-1}, χ^3_{-1}, ... being zero. Substituting the expansion for ξ_0 in (14*b*) and collecting terms up to the first order in α^{-1}, we get

$$-\frac{\partial}{\partial\theta}\xi^0_0 = r\cos\theta, \quad \xi^0_0 - \frac{\partial}{\partial\theta}\xi^1_0 = 0. \tag{42a, b}$$

Differentiating (42*b*) with respect to θ and using (42*a*), we obtain

$$\frac{\partial^2}{\partial\theta^2}\xi^1_0 = -r\cos\theta, \tag{43}$$

which is solved by

$$\xi^1_0 = r\cos\theta. \tag{44}$$

This solution is not unique. Indeed, any function $\hat{\xi}^1_0(r)$ depending only on r could be added. Here we choose this arbitrary function to be zero. No matter, however, which choice we make for $\hat{\xi}^1_0(r)$, if we substitute the results back into (42*b*), we find

$$\xi^0_0 = -r\sin\theta, \tag{45}$$

which solution satisfies (42*a*). Note that by considering (42*a*) and (42*b*) in conjunction, the only indeterminacy is in ξ^1_0. The streamfunctions χ^0_0 and χ^1_0 are

$$\chi^0_0 = -\tfrac{1}{8}(r^2-1)\,r\sin\theta, \quad \chi^1_0 = \tfrac{1}{8}(r^2-1)\,r\cos\theta. \tag{46a, b}$$

Continuing with the next order, we get the following set of equations:

$$-\frac{\partial}{\partial\theta}\xi^0_1 = -J(\chi^0_0, \xi^0_0 + y), \tag{47a}$$

$$\xi^0_1 - \frac{\partial}{\partial\theta}\xi^1_1 = -J(\chi^0_0, \xi^1_0) - J(\chi^1_0, \xi^0_0 + y). \tag{47b}$$

Because $\xi^0 + y = 0$, these equations can be simplified to

$$\frac{\partial}{\partial\theta}\xi^0_1 = 0, \quad \xi^0_1 - \frac{\partial}{\partial\theta}\xi^1_1 = -J(\chi^0_0, \xi^1_0). \tag{48a, b}$$

For the Jacobian on the right-hand side of (48*b*) we have

$$J(\chi^0_0, \xi^1_0) = \tfrac{1}{8}[2r^2 - 1 - r^2\cos 2\theta]. \tag{49}$$

Differentiating (48*b*) with respect to θ and using (48*a*) together with expression (49) for the Jacobian, we get

$$\frac{\partial^2}{\partial\theta^2}\xi^1_1 = \tfrac{1}{4}r^2\sin 2\theta. \tag{50}$$

The solution, unique up to an arbitrary term $\hat{\xi}_1^1(r)$, is

$$\xi_1^1 = -\tfrac{1}{16}r^2 \sin 2\theta. \tag{51}$$

No matter which choices we make for $\hat{\xi}_0^1(r)$ and $\hat{\xi}_1^1(r)$, if we substitute the corresponding expression back into (48*b*) and use again (49), we obtain

$$\xi_1^0 = -\tfrac{1}{8}(2r^2 - 1), \tag{52}$$

which solution satisfies (48*a*). For the streamfunctions associated with ξ_1^0 and ξ_1^1 we have

$$\chi_1^0 = -\tfrac{1}{64}(r^2-1)(r^2-1), \quad \chi_1^1 = -\tfrac{1}{192}(r^2-1)r^2 \sin 2\theta. \tag{53a, b}$$

The expressions for ξ_{-1}^0, ξ_{-1}^1, ξ_0^0, ξ_0^1, etc. and the accompanying streamfunctions are in accordance with the general expression given in §2.3. This can be verified by first applying (15) and expanding the results in powers of α^{-1}.

We next consider the case for a general value of $k \geqslant 1$. For the kth equation of (14) we have, retaining terms up to the first order in the expansion in α^{-1},

$$\frac{\partial}{\partial\theta}\xi_k^0 = I_k, \quad \xi_k^0 - \frac{\partial}{\partial\theta}\xi_k^1 = -J_k, \tag{54a, b}$$

where I_k and $J_k (k \geqslant 1)$ are given by

$$I_k = J(\chi_0^0, \xi_{k-1}^0) + \ldots + J(\chi_{k-1}^0, \xi_0^0 + y), \tag{55a}$$

$$J_k = J(\chi_0^0, \xi_{k-1}^1) + \ldots + J(\chi_{k-1}^0, \xi_0^1) + J(\chi_0^1, \xi_{k-1}^0) + \ldots + J(\chi_{k-1}^1, \xi_0^0 + y). \tag{55b}$$

We recall that our previous analysis has shown that $\xi_0^0 + y = 0$. This simplifies expressions (55) somewhat as it implies, in particular, that $I_1 = 0$. Differentiating (54*b*) with respect to θ and then substituting (54*a*), gives

$$\frac{\partial^2}{\partial\theta^2}\xi_k^1 = I_k + \frac{\partial}{\partial\theta}J_k. \tag{56}$$

A solution is obtained by integrating twice with respect to θ (concerning the integral operator, see also §A 1 of the Appendix):

$$\xi_k^1 = \int^\theta \int^\theta I_k + \int^\theta \int^\theta \frac{\partial}{\partial\theta}J_k. \tag{57}$$

Again, the solution is unique up to an arbitrary term $\hat{\xi}_k^1(r)$. Furthermore, the integration with respect to θ is only possible if I_k does not contain terms which depend only on r. We now assume that the field I_k does not contain such terms. (This assumption should, in fact, be proven but calculations with the formula manipulation package *Mathematica* have shown that it is true for at least 20 orders in the δ^{-1} expansion.) No matter which choice we make for $\hat{\xi}_k^1$, we obtain for ξ_k^0 after substituting (57) into (54*b*)

$$\xi_k^0 = \int^\theta I_k + \int^\theta \frac{\partial}{\partial\theta}J_k - J_k. \tag{58}$$

This expression solves (54*a*). Note that the first term on the right-hand side of (58) does not contain terms that only depend on r. The second and third terms together, on the other hand, only give terms that depend on r. Equations (57) and (58), together with (55) are the basis of our calculation of ξ^0 and ξ^1 and the corresponding streamfunctions χ^0 and χ^1.

We conclude this subsection by discussing a few examples. Using the spectral method, described in the Appendix, we calculated ξ_k^0 and ξ_k^1 up to $k = 50$. The series expansion of ξ_k^0 converges uniformly if $\ln\delta > -0.94$, whereas the expansion of ξ_k^1 converges uniformly if $\ln\delta > -0.93$, as has been established in the manner discussed in the Appendix. In figures 5(*a*) and 5(*b*) we show three examples of solutions calculated in the manner described – summing all terms in (39) up to $k = 50$. The values of δ are $\ln\delta = 0.25$, -0.25 and -0.75 (first, second and third column in figure 5*a*). In the figure we show the absolute vorticity $\xi^0 + y$ (first row), the relative vorticity ξ^0 (second row), the streamfunction χ^0 (third row) and a scatter diagram of $\xi^0 + y$ against χ^0 (fourth row). The third column of this figure should be compared with the third column of figure 4, where the solution for the same value of δ is shown but with a large though finite value of α. Notice that the scatter diagrams clearly demonstrate that we obtained truly free mode solutions of (33*a*) with a single functional relationship between $\xi^0 + y$ and χ^0. Notice also that the functional relationships are slightly nonlinear and that they become more nonlinear if δ becomes smaller. In figure 5(*b*) we show for the same three values of δ (the three different columns) the solutions for ξ^1 (first row) and χ^1 (second row). The fact that we found these solutions implies that the basic free mode solutions of (33*a*) satisfy the Niiler–Pierrehumbert–Malguzzi integral criterion. Indeed, this criterion is a necessary condition for (33*b*) to be solvable. Because we actually solved that equation, the condition must be satisfied. We notice that this favourable state of affairs is the result of considering (33*a*) and (33*b*) at the same time.

As to the symmetry properties of the free mode and the almost free correction we observe the following. The free mode has a symmetry axis that runs north–south. Around the east–west axis the symmetry is broken in that the circulation is stronger on the northern side, reminiscent of the northern boundary layer in a Fofonoff mode. Indeed, as was first noted by Høiland (1950), any flow on a rotating sphere with closed streamlines that conserves absolute vorticity must show this basic asymmetry. Here we see that the asymmetry is already established by the first two terms in the series expansion of the free mode, i.e. the sum $\delta\chi_{-1}^0 + \chi_0^0$ (41*a*) and (46*a*)). Note that the strength of the symmetry breaking is given by δ^{-1}. This is the equivalent of the establishment of an inertial boundary layer if $\delta \to 0$, when δ becomes the dimensionless width of the boundary layer. By definition of δ this width is a function of forcing and damping. Thus our δ is the same parameter as the inferred dimensionless thickness of the inertio-frictional boundary layer as given by Niiler (1966). (For a full appreciation of this role of δ we refer to the latter reference or to Zimmerman & Maas 1989.) Note also that just as in the limit of strong forcing in the Veronis sequence, the planetary vorticity gradient is annihilated by the gradient of the ξ_0^0 field. Around the north–south axis the symmetry of the free mode will actually be broken by the almost free correction which is antisymmetric around the north–south axis. Thus, in the presence of weak forcing and friction the flow is slightly reinforced on the west side and weakened on the east side. Also this corroborates the result of Niiler (1966).

5. The absolute vorticity versus streamfunction relationship

As has been noted before, the specific absolute vorticity versus streamfunction relationship is a subject of central concern in geophysical fluid dynamics. In ocean circulation theory a question that often arises is whether a quasi-inertial gyre approaches the Fofonoff mode, i.e. an inertial circulation with a linear functional relationship between absolute vorticity and streamfunction. That the inertial mode

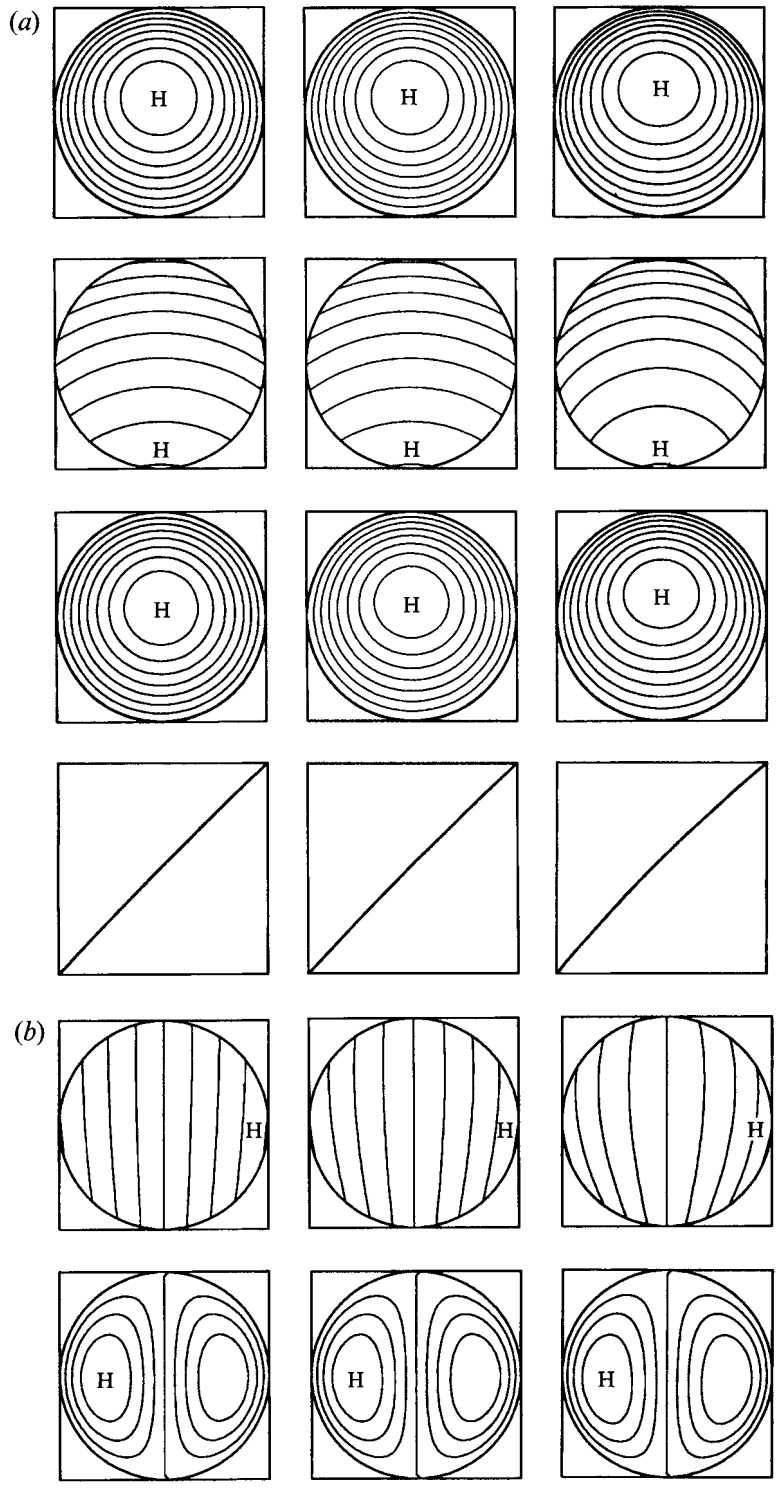

FIGURE 5. (*a*) The absolute vorticity ξ^0+y (first row), the relative vorticity ξ^0 (second row), the streamfunction χ^0 (third row) and a scatter diagram (fourth row) of ξ^0+y against χ^0 of the solution in the inertial limit, calculated using the series expansion in δ^{-1} up to $k = 50$. In the first column the value of $\ln\delta$ is 0.25, in the second $\ln\delta$ is -0.25 and in the last $\ln\delta$ is -0.75. The fields in the third

	0	1	2	3	4	5
0	-2	$-\frac{1}{2^3}$	$\frac{1}{3\times 2^9}$	$-\frac{1}{3\times 2^{14}}$	$\frac{47}{3^2\times 2^{21}}$	$-\frac{11\times 61}{5\times 3^2\times 2^{26}}$
1		$\frac{1}{2}$	$\frac{3}{2^7}$	$\frac{3}{2^{13}}$	$\frac{1}{5\times 3\times 2^{18}}$	$-\frac{541}{5\times 3^2\times 2^{25}}$
2			$-\frac{3}{2^6}$	$-\frac{3}{2^9}$	$-\frac{233}{3\times 2^{18}}$	$-\frac{449}{5\times 3\times 2^{22}}$
3				$\frac{5}{2^9}$	$\frac{31\times 37}{3^2\times 2^{16}}$	$\frac{23801}{5\times 3^2\times 2^{20}}$
4					$-\frac{17\times 5}{2^{15}}$	$-\frac{7\times 3169}{5\times 3\times 2^{21}}$
5						$\frac{13\times 14033}{5^2\times 3^2\times 2^{20}}$

TABLE 2. A few values of the coefficients a_{00}, a_{01}, etc., calculated in the manner described in §5 and using the formula manipulation package *Mathematica*. The value of a_{ij} is placed on the ith row and in the jth column.

should have such a linear relationship has sometimes been inferred from a result of equilibrium statistical mechanics of two-dimensional flow. If one maximizes a suitably defined macroscopic entropy under the constraints of a fixed circulation, energy and potential enstrophy one obtains as the most probable state a flow configuration that is characterized by a linear relationship between absolute vorticity and streamfunction (e.g. Salmon, Holloway & Hendershott 1976). The consideration of only circulation, energy and potential enstrophy as constraints is then loosely supported by viscous dissipation of the other conserved quantities at small scales. This argument forms the basis of Holloway's (1986) suggestion that in the weakly dissipative cases studied by Merkine *et al.* (1985) the Fofonoff mode is emerging despite forcing and dissipation.

In principle, the restriction to only three constraints in a statistical mechanical approach is unnecessary. Indeed, recent work on the statistical mechanics of geophysical fluid flow (Robert & Sommeria 1991; Miller, Weichman & Cross 1992) has shown that it is possible to formulate a statistical mechanical theory that takes into account all other conserved quantities of the inviscid system (e.g. all other powers of the absolute vorticity integrated over the flow domain). If all invariants are properly dealt with, in general a nonlinear relationship between absolute vorticity and streamfunction will be the result. Without wanting to suggest any direct connection of these results with ours we shall nonetheless show that also for the problem we deal with here the functional relationship between absolute vorticity and streamfunction is in general a nonlinear one, determined by the ratio δ of the (vanishingly small) forcing and friction terms. The latter result corroborates the conclusion of Merkine *et al.* (1985) that, if nearly inviscid steady states are possible, the functional relationships between their absolute vorticity and streamfunction are determined by the (vanishingly small) forcing and friction terms.

column should be compared with those of the third column in figure 4, where the solution is shown for the same value of δ but with a large though finite value of α. (*b*) The relative vorticity ξ^1 (first row) and the streamfunction χ^1 (second row) of the almost free correction, calculated using the series expansion in δ^{-1} up to $k = 50$. In the first column the value of $\ln\delta$ is 0.25, in the second $\ln\delta$ is -0.25 and in the last $\ln\delta$ is -0.75.

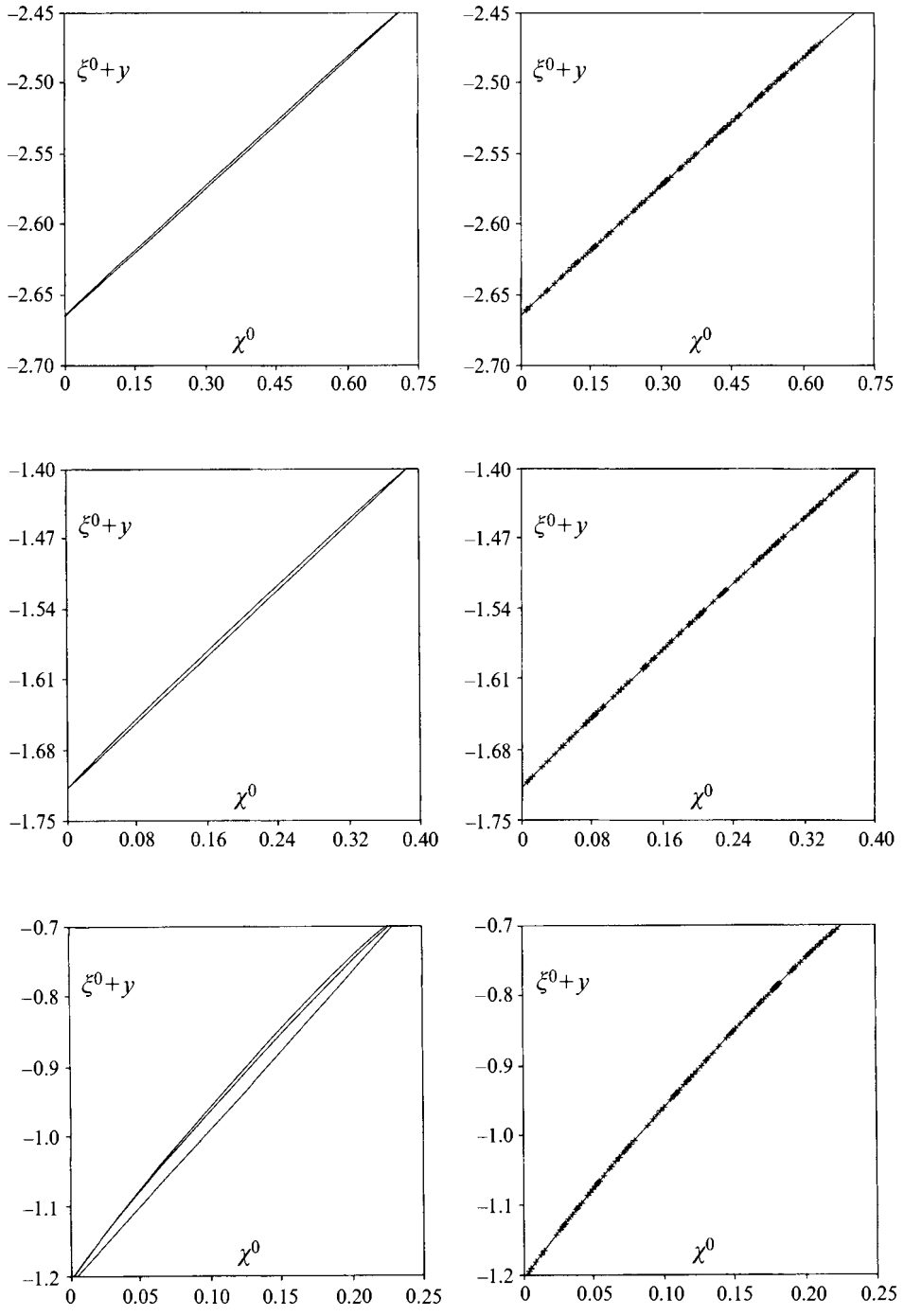

FIGURE 6. Left column: the functional relationship (76) between ξ^0+y and χ^0 with the coefficients a_0, a_1, etc. in (65) up to order δ^{-2} (giving a linear relationship), up to order δ^{-4} (giving a quadratic relationship) and up to order δ^{-6} (giving a cubic relationship). In the upper row the value of $\ln\delta$ is 0.25, in the middle row $\ln\delta$ is -0.25 and in the last row $\ln\delta$ is -0.75. Right column: the functional relationship (76) between ξ^0+y and χ^0 with the coefficients a_0, a_1, etc. in (65) up to order δ^{-6} (giving a cubic relationship), together with the scatter diagrams of figure 5(*a*) corresponding to the same

In analysing the functional relationship between the absolute vorticity ξ^0+y and the streamfunction χ^0 in the inertial limit, we may study these fields on any smooth curve that crosses the streamlines. It turns out to be convenient to choose the line $\theta = 0$ and $0 \leqslant r \leqslant 1$. In the expansions of ξ^0+y and χ^0 we then only need to consider terms of the form $r^n \cos m\theta$. Furthermore, because ξ^0+y and χ^0 were seen to be symmetric around the axis $x = 0$, there will be no terms of the form $r^n \cos m\theta$ with m odd. So, we only have to study terms in the expansion of the form $r^n \cos m\theta$ with m even. Now, it follows from the general properties of the series expansion in δ^{-1}, as given in §2.3, that in the expansions (39)

$$\xi^0+y = \delta\xi^0_{-1}+\xi^0_0+y+\delta^{-1}\xi^0_1+\delta^{-2}\xi^0_2+\ldots, \tag{59a}$$

$$\chi^0 = \delta\chi^0_{-1}+\chi^0_0+\delta^{-1}\chi^0_1+\delta^{-2}\chi^0_2+\ldots \tag{59b}$$

only the fields ξ^0_{-1}, ξ^0_1, ξ^0_3, etc. and χ^0_{-1}, χ^0_1, χ^0_3, etc. contribute terms $r^n \cos m\theta$ with m even. So, if we define

$$q(r) \equiv \delta^{-1}(\xi^0+y), \quad p(r) \equiv \delta^{-1}\chi^0, \tag{60a, b}$$

where ξ^0+y and χ^0 are evaluated in $(r, \theta = 0)$, we can write

$$q(r) = q_0(r)+\delta^{-2}q_1(r)+\delta^{-4}q_2(r)+\ldots, \tag{61a}$$

$$p(r) = p_0(r)+\delta^{-2}p_1(r)+\delta^{-4}p_2(r)+\ldots, \tag{61b}$$

where

$$q_l(r) \equiv \xi^0_{2l-1}, \quad p_l(r) \equiv \chi^0_{2l-1}, \tag{62a, b}$$

evaluated in $(r, \theta = 0)$. In §2.3 it also mentioned that the vorticity fields in the order-k contribution are elements of $T(k+1)$ and that the streamfunction fields are elements of $T(k+3)$ with $|m| \leqslant k+1$. In the light of the foregoing this means that

$$q_l(r) = q_{l0}+r^2q_{l1}+\ldots+r^{2l}q_{ll}, \tag{63a}$$

$$p_l(r) = p_{l0}+r^2p_{l1}+\ldots+r^{2l}p_{ll}+r^{2l+2}p_{ll+1}, \tag{63b}$$

i.e. q_l is a power series in r^2 with degree l and p_l is a power series in r^2 with degree $l+1$.

We now conjecture that q can be written as a power series in p, i.e.

$$q(r) = a_0+a_1p(r)+a_2[p(r)]^2+a_3[p(r)]^3+\ldots, \tag{64}$$

where a_0, a_1, a_2, etc. are power series in δ^{-2} of the form

$$a_0 = a_{00}+\delta^{-2}a_{01}+\delta^{-4}a_{02}+\delta^{-6}a_{03}+\ldots, \tag{65a}$$

$$a_1 = \delta^{-2}a_{11}+\delta^{-4}a_{12}+\delta^{-6}a_{13}+\delta^{-8}a_{14}+\ldots, \tag{65b}$$

$$a_2 = \delta^{-4}a_{22}+\delta^{-6}a_{23}+\delta^{-8}a_{24}+\delta^{-10}a_{25}+\ldots, \tag{65c}$$

$$\vdots$$

Substituting (61) and (65) into (64) we get

$$\begin{aligned} q_0+\delta^{-2}q_1+\delta^{-4}q_2+\ldots = {} & a_{00}+\delta^{-2}a_{01}+\delta^{-4}a_{02}+\ldots \\ & +[\delta^{-2}a_{11}+\delta^{-4}a_{12}+\ldots][p_0+\delta^{-2}p_1+\delta^{-4}p_2+\ldots] \\ & +[\delta^{-4}a_{22}+\delta^{-6}a_{23}+\ldots][p_0+\delta^{-2}p_1+\delta^{-4}p_2+\ldots]^2 \\ & +[\delta^{-6}a_{33}+\delta^{-8}a_{34}+\ldots][p_0+\delta^{-2}p_1+\delta^{-4}p_2+\ldots]^3+\ldots. \end{aligned} \tag{66}$$

Collecting terms of like order in δ^{-2}, we obtain for the δ^{-2}-independent contribution

$$q_0 = a_{00}. \tag{67}$$

As q_0 only consists of the constant term q_{00} we get

$$a_{00} = q_{00}. \tag{68}$$

values of δ. The figure shows that the cubic functional relationship already gives an almost perfect fit to the points.

Equating the δ^{-2}-order terms we obtain

$$q_1 = a_{01} + a_{11} p_0, \tag{69}$$

which gives, when combined with (63),

$$q_{10} + r^2 q_{11} = a_{01} + a_{11}(p_{00} + r^2 p_{01}). \tag{70}$$

Equating like powers of r^2 gives two linear equations in the two unknowns a_{01} and a_{11}. The solution is

$$a_{01} = q_{10} - \frac{p_{00}}{p_{01}} q_{11}, \quad a_{11} = \frac{q_{11}}{p_{01}}. \tag{71a, b}$$

For the next order in δ^{-2} we have

$$q_2 = a_{02} + a_{11} p_1 + a_{12} p_0 + a_{22} p_0^2, \tag{72}$$

or, after substituting (63),

$$\begin{aligned} q_{20} + r^2 q_{21} + r^4 q_{22} = {} & a_{02} + a_{11}(p_{10} + r^2 p_{11} + r^4 p_{12}) \\ & + a_{12}(p_{00} + r^2 p_{01}) + a_{22}(p_{00}^2 + 2r^2 p_{00} p_{01} + r^4 p_{01}^2). \end{aligned} \tag{73}$$

Equating like powers of r^2 gives a system of three linear equations in the three unknowns a_{02}, a_{12} and a_{22}. Closer inspection of (66) shows that the pattern repeats itself: equating the δ^{-6} terms leads to four linear equations in four unknowns, equating the δ^{-8} terms leads to five linear equations in five unknowns, etc.

The analysis above shows that the coefficients a_{00}, a_{01}, a_{02}, etc. in (65) can be found in a systematic way. For the coefficients a_{00}, a_{01} and a_{11} we can use the expressions in §4.2 to obtain their values. Indeed, it follows from (40*a*) (41*a*), (52) and (53*a*) that

$$q_{00} = -2, \quad q_{10} = \tfrac{1}{8}, \quad q_{11} = \tfrac{1}{4}; \quad p_{00} = \tfrac{1}{2}, \quad p_{01} = -\tfrac{1}{2}, \tag{74a, b}$$

which gives for a_{00}, a_{01} and a_{11}

$$a_{00} = -2, \quad a_{01} = -\tfrac{1}{8}, \quad a_{11} = \tfrac{1}{2}. \tag{75}$$

The other coefficients can be found in a similar way. Using the formula manipulation package *Mathematica* we calculated a few more coefficients, which are given in table 2.

Since our series solution for the free mode obeys (33*a*), the functional relationship (64) must hold for all other points in the domain. Substituting (60) in (64) and multiplying the left-and right-hand sides by δ gives

$$\xi^0 + y = \delta a_0 + a_1 \chi^0 + \delta^{-1} a_2 [\chi^0]^2 + \delta^{-2} a_3 [\chi^0]^3 + \ldots, \tag{76}$$

where the coefficients a_0, a_1, a_2, etc. are given by (65) and a few of the numbers a_{00}, a_{01}, etc. are given in table 2. In the left column of figure 6 we show the functional relationship with the coefficients a_0, a_1, etc. up to order δ^{-2} (linear), up to order δ^{-4} (quadratic), and up to order δ^{-6} (cubic) for $\ln \delta = 0.25$, -0.25 and -0.75. These values of δ are the same as those corresponding with the cases in figure 5. In the right column of figure 6 we show the cubic functional relationship for these three cases together with the scatter plots as shown in figure 5(*a*). We see that already for the cubic relationship the points of the scatter diagram neatly fall on the calculated functional relationships.

We can now use the result (76) in order to establish the physical condition for which the functional relationship between absolute vorticity and streamfunction tends asymptotically to a linear one. As is evident from the structure of the coefficients a_0, a_1, etc., this is the case if $\delta \to \infty$. Now in terms of dimensional quantities (§2) we have

$$\delta = \frac{\tau_*}{2\beta R \kappa_*} \propto \frac{T_R}{T_C}, \tag{77}$$

where $T_R = 1/\beta R$ is the period of the gravest Rossby wave and $T_C = \kappa_*/\tau_*$ is the circulation timescale of the gyre. Physically then a linear functional relationship between absolute vorticity and streamfunction applies if the circulation timescale is much smaller than the period of the gravest Rossby wave. Conversely, a small δ, as in a circulation with a genuine inertial boundary layer, will result in a strongly nonlinear functional relationship.

6. Summary and conclusions

We have shown that in the strongly nonlinear limit, i.e. a large value of the parameter α as defined in (5), a wind-driven ocean gyre may be in two distinct modes which are only superficially similar. If one keeps the Ekman number (friction) fixed and increases the Rossby number (forcing) one encounters the strongly forced limit. The circulation becomes asymptotically circularly symmetric with a relatively weak dipolar perturbation. The dominant circularly symmetric contribution is proportional to α whereas the dipolar contribution is independent of α. The latter contribution breaks the circular symmetry such that the remaining symmetry of the circulation pattern is around the north–south axis. The dipolar perturbation has a relative vorticity field that varies linearly with the north–south coordinate and that exactly annihilates the planetary vorticity gradient. In this limit there is no unique relationship between absolute vorticity and streamfunction, proving that this limit is certainly not an inertial one. It is this limit that is the strongly nonlinear asymptote of the numerical simulation sequence of Veronis (1966*b*).

The second strongly nonlinear limit is obtained by having asymptotically vanishing Rossby and Ekman numbers while at the same time having α approaching infinity. The latter can be realized by having a constant ratio of the Rossby and Ekman number and then letting both go to zero since α is proportional the ratio of the Rossby number and the squared Ekman number. The circulation obtained in that regime is a genuine inertial circulation. It shares two features with the limit of strong forcing: a north–south symmetry axis and annihilation of the planetary vorticity gradient. However, it does have a unique relationship between absolute vorticity and streamfunction, which is in general a nonlinear one. Only when the circulation time is greatly exceeded by the period of the gravest Rossby wave is the relationship asymptotically linear.

The establishment of a unique functional relationship in the inertial limit is closely related to a solvability condition for the free mode in terms of the almost free correction, as was first formulated by Niiler (1966) and Pierrehumbert & Malguzzi (1984). It is a point of strength of our perturbation series that it is able to give more than just a formal condition for the solution of the free mode, but that it produces in series form a closed solution both for the free mode and for the almost free correction. From that solution the functional relationship can be obtained as the absolute vorticity in terms of a power series in the streamfunction.

The work described in this paper originated when one of the authors (W.T.M.V.) held a postdoctoral position at the Netherlands Institute for Sea Research and was completed during his subsequent affiliation with the Royal Netherlands Meteorological Institute. The support given by both institutes is gratefully acknowledged. This investigation was supported (in part) by the Working Group on Meteorology and Physical Oceanography (MFO) with financial aid from the Netherlands Organization

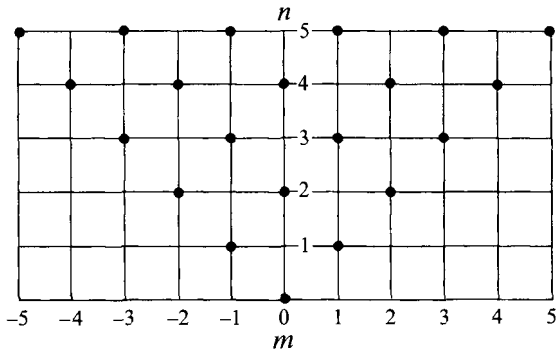

FIGURE 7. Graphical representation of the functions $X_{mn}(r,\theta) \equiv r^n e^{im\theta}$. Each dot, with coordinates m and n, is to be associated with one function X_{mn}. Note that the n-values increase in steps of two. The dots shown in this figure represents the space $T5$.

for Scientific Research (NWO). We thank Dr L. R. M. Maas for his comments on the first draft of this paper.

Appendix. A spectral method to solve the equations

In this Appendix we will demonstrate how the hierarchies of equations that appeared in the foregoing sections can be solved systematically to any order in κ^{-1} or δ^{-1}. For convenience we limit ourselves to the series expansion (7) and the hierarchy of equations (11), but everything that follows holds equally well for (13) and (14) and for the different limiting cases. To explain the method we start by introducing the functions

$$X_{mn}(r,\theta) \equiv r^n e^{im\theta}, \tag{A 1}$$

where $m = \ldots -2, -1, 0, 1, 2, \ldots$ and $n = |m| + 2p$ with $p = 0, 1, 2, \ldots$. If $-N \leqslant m \leqslant N$ and $n \leqslant N$ these functions span the same linear vector space as $1, x, y, x^2, xy, y^2, \ldots, x^N, x^{N-1}y, \ldots, xy^{N-1}, y^N$. The space spanned by the functions (A 1) for a finite value of N is denoted by TN. The functions X_{mn} can be represented conveniently by a diagram in which each function is denoted by a dot in a lattice of which the coordinates are m and n, see figure 7. The T in this notation, in analogy to the usage in spectral models for a sphere based on spherical harmonics, refers to the triangular shape of the lattice of points representing the functions in figure 7. (This figure represents a $T5$ truncation.) Any field η that belongs to TN can be written as

$$\eta = \sum_{m=-N}^{N} \sum_{n=|m|}^{N} \eta_{mn} X_{mn}, \tag{A 2}$$

where, as $n = |m| + 2p$, the summation over n involves $|m|$, $|m|+2, \ldots$, etc. The coefficients η_{mn} are usually complex and can be written as

$$\eta_{mn} = \eta^r_{mn} + i\eta^i_{mn}, \tag{A 3}$$

where η^r_{mn} is the real part of η_{mn} and η^i_{mn} is the imaginary part. In order for the field η to be real, we should have that

$$\eta_{-mn} = \eta^*_{mn}, \tag{A 4}$$

where the asterisk denotes complex conjugate.

A.1. *Representation of the operators*

To explain how the functions X_{mn} can be used to solve the equations (11), (14) or their limiting cases (24) and (54)–(58), we consider the action of the operators appearing in these equations. These operators are the derivative $\partial/\partial\theta$, $(1-\alpha\partial/\partial\theta)$, $(\alpha^{-1}-\partial/\partial\theta)$, the Laplacian ∇^2 as well as their inverses and the Jacobian. Let us first consider the operator $\partial/\partial\theta$ and its inverse $\int^\theta$. We note that the derivative operator acting on a field that only depends on r yields zero. As a consequence, the integral operator is only defined for arguments that do not contain fields that only depend on r. In addition, there is some arbitrariness in the action of the integral operator as any field that depends only on r could be added to the result. In our definition of the integral operator we set this arbitrary field equal to zero. So, the action of the operators $\partial/\partial\theta$ and $\int^\theta$ on the functions X_{mn} is given by

$$\frac{\partial}{\partial\theta}X_{mn} = \mathrm{i}mX_{mn}, \quad \int^\theta X_{mn} = (\mathrm{i}m)^{-1}X_{mn}. \tag{A 5a, b}$$

These expressions make explicit that if η belongs to TN, then $\partial\eta/\partial\theta$ belongs to the subspace of TN with $m=0$ excluded. Furthermore, $\int^\theta\eta$ is only defined if the representation of η does not contain terms with $m=0$. From the expressions above it follows for the representations that

$$\left[\frac{\partial\eta}{\partial\theta}\right]_{mn} = \mathrm{i}m\eta_{mn}, \quad \left[\int^\theta\eta\right]_{mn} = (\mathrm{i}m)^{-1}\eta_{mn}, \tag{A 6a, b}$$

where $[\ldots]_{mn}$ denotes the coefficients of the field between brackets. For any operator of the form $(a+b\,\partial/\partial\theta)$ and its inverse $(a+b\,\partial/\partial\theta)^{-1}$ we have

$$\left(a+b\frac{\partial}{\partial\theta}\right)X_{mn} = (a+\mathrm{i}mb)\,X_{mn}, \tag{A 7a}$$

$$\left(a+b\frac{\partial}{\partial\theta}\right)^{-1}X_{mn} = (a+\mathrm{i}mb)^{-1}\,X_{mn}. \tag{A 7b}$$

If $a\neq 0$ these operators leave the space TN invariant. From the expressions above it is easily deduced that

$$\left[\left(a+b\frac{\partial}{\partial\theta}\right)\eta\right]_{mn} = (a+\mathrm{i}mb)\,\eta_{mn}, \tag{A 8a}$$

$$\left[\left(a+b\frac{\partial}{\partial\theta}\right)^{-1}\right]_{mn} = (a+\mathrm{i}mb)^{-1}\,\eta_{mn}. \tag{A 8b}$$

It can be verified from (2) and (A 1) that for the Laplace operator ∇^2 and its inverse ∇^{-2} we have

$$\nabla^2 X_{mn} = (n^2-m^2)\,X_{mn-2}, \tag{A 9a}$$

$$\nabla^{-2}X_{mn} = ((n+2)^2-m^2)^{-1}(X_{mn+2}-X_{m|m|}). \tag{A 9b}$$

These expressions show that if η belongs to TN then $\nabla^2\eta$ belongs to $T(N-2)$ and $\nabla^{-2}\eta$ belongs to $T(N+2)$ with $|m|\leqslant N$. It can be deduced from (A 9) that we have

$$[\nabla^2\eta]_{mn} = ((n+2)^2-m^2)\,\eta_{mn+2}, \tag{A 10a}$$

$$[\nabla^{-2}\eta]_{mn} = \sum_{n'=|m|+2}^{N+2}(n'^2-m^2)^{-1}(\delta_{nn'}-\delta_{n|m|})\,\eta_{mn'-2}. \tag{A 10b}$$

We note that $\nabla^{-2}\eta$, being the streamfunction associated with η, should obey the boundary condition $\nabla^{-2}\eta = 0$ at $r = 1$. The coefficients $[\nabla^{-2}\eta]_{mn}$ should therefore satisfy

$$\sum_{n=|m|}^{N+2} [\nabla^{-2}\eta]_{mn} = 0 \tag{A 11}$$

for all values of m for which $|m| \leqslant N$. This condition follows directly from the fact that the r-dependent part of the functions X_{mn} is 1 at $r = 1$. It can be checked that (A 10b) is in accordance with this condition. Furthermore, the Laplace operator is supposed to act only on fields that satisfy this condition.

We now discuss the method by means of which the Jacobians are calculated. Let us consider two fields η and σ, where η (a streamfunction) belongs to $T(M+2)$ with $|m| \leqslant M$ and σ (a vorticity field) belongs to TN. The coefficients of these fields are η_{mn} and σ_{mn}, respectively. For the Jacobian of η and σ we can write

$$J(\eta, \sigma) = \sum_{m=-M}^{M} \sum_{n=|m|}^{M+2} \sum_{m'=-N}^{N} \sum_{n'=|m'|}^{N} \eta_{mn}\, \sigma_{m'n'} J(X_{mn}, X_{m'n'}). \tag{A 12}$$

From the definition of the Jacobian and the functions X_{mn} it can be verified that

$$J(X_{mn}, X_{m'n'}) = \mathrm{i}(nm' - n'm)\, X_{(m+m')\,(n+n'-2)}. \tag{A 13}$$

From (A 13) it can be seen that the Jacobian of η and σ belongs to the space $T(M+N)$ and can therefore be written as

$$J(\eta, \sigma) = \sum_{m=-(M+N)}^{M+N} \sum_{n=|m|}^{M+N} J_{mn} X_{mn}. \tag{A 14}$$

By writing (A 13) formally as

$$J(X_{mn}, X_{m'n'}) = \sum_{m''=-(M+N)}^{M+N} \sum_{n''=|m''|}^{M+N} \mathrm{i}(nm' - n'm)\, \delta_{(m+m')\,m''} \delta_{(n+n'-2)\,n''} X_{m''n''}, \tag{A 15}$$

we obtain for J_{mn} the expression

$$J_{mn} = \sum_{m'=-M}^{M} \sum_{n'=|m|}^{M+2} \sum_{m''=-N}^{N} \sum_{n''=|m''|}^{N} \mathrm{i}(n'm'' - n''m')\, \delta_{m(m'+m'')}\, \delta_{n(n'+n''-2)}\, \eta_{m'n'}\, \sigma_{m''n''}. \tag{A 16}$$

In principle the quadruple summation in (A 16) can be reduced to a double summation. In our calculations we did not use that possibility.

A.2. *General properties of the series*

We will next show that the fields ζ_k and ψ_k that result from solving the kth equation (11) have the following properties. First, ζ_k is an element of $T(k+1)$ and, consequently, the field ψ_k is an element of $T(k+3)$ with $|m| \leqslant k+1$. Secondly, for even k the fields ζ_k and ψ_k are expressed in functions X_{mn} with odd m and for odd k the fields ζ_k and ψ_k only contain functions X_{mn} with even m. The proofs are by induction. Let us start with the first property. From inspection of (9), (16) and (18) it can be seen that the statement is certainly true for $k = -1, 0$ and 1. Let us assume it is true for all k-values less than some value $l-1$. To prove that it is also true for $k = l$ we note that the Jacobians in (11) have the general form $J(\psi_i, \zeta_{l-i-1})$ with $i = 0, 1, \ldots, l-1$. Now, because ψ_i is the streamfunction associated with ζ_i it will be, by assumption, an element of $T(i+3)$ with $|m| \leqslant i+1$. By the same assumption ζ_{l-i-1} will be an element of $T(l-i)$. From the discussion above on the calculation of the Jacobian it can then be seen that $J(\psi_i, \zeta_{l-i-1})$ is an element of $T(l+1)$, independent of i. So the whose source term in the lth equation (11) is an element of $T(l+1)$. As the operator $(1-\alpha\partial/\partial\theta)^{-1}$ leaves the space $T(l+1)$ invariant the resulting ζ_l will also be an element of $T(l+1)$ and ψ_l will

therefore be an element of $T(l+3)$ with $|m| \leqslant l+1$, which completes the proof. The second property can also be proven by induction. Inspection of (9), (16) and (18) shows again that the statement is true for $k = -1$, 0 and 1. Let us assume that it is true for all k-values less than some value $l-1$ and let us first assume that l is even. Owing to the general form $J(\psi_i, \zeta_{l-i-1})$ with $i = 0, 1, \ldots, l-1$ of the Jacobians in (11), we have that for even as well as odd i the Jacobians in (11) only contain functions X_{mn} with m odd. This follows from the induction assumption and property (A 13) of the Jacobian. Now, as the operator $(1-\alpha\partial/\partial\theta)^{-1}$ does not change functions X_{mn} with odd m into functions X_{mn} with even m or vice versa, the resulting field ζ_l will only contain functions X_{mn} with odd m. This proves the conjecture for even l. In the same way the conjecture can be proven for odd l.

A.3. *Convergence of the series*

The procedure we have used in solving the hierarchy of equations (11) can now be described as follows. The field ζ_{-1} and corresponding ψ_{-1} are directly given by (9). The next field ζ_0 is obtained by applying $(1-\alpha\partial/\partial\theta)^{-1}$ to $\alpha x = \alpha r\cos\theta$, using (A 7*b*). The corresponding ψ_0 is calculated by using (A 10*b*). Then the Jacobian term $-J(\psi_0, \zeta_0+y)$ is calculated by means of (A 16) after which, in the same manner as described above, $(1-\alpha\partial/\partial\theta)^{-1}$ is applied to the result, giving ζ_1. Then ψ_1 is calculated by means of (A 10*b*) and the procedure is repeated up to the desired order.

Using the method described above we solved the hierarchies of equations up to $k = 50$. Because the results are only relevant if the series for ζ and ψ converge, we consider the convergence properties, in particular the convergence of ζ. Define M_k to be the maximum absolute value of ζ_k. Then, according to Rudin (1964, p. 134) the series (7*a*) for ζ converges uniformly if

$$M = \kappa M_{-1} + M_0 + \kappa^{-1}M_1 + \kappa^{-2}M_2 + \ldots \tag{A 17}$$

converges. Expression (A 17) is a power series in κ^{-1} and, according to Rudin (1964, p. 60), this series converges if κ is larger than the inverse radius of convergence ρ defined by

$$\rho \equiv \limsup_{k\to\infty} M_k^{1/k}. \tag{A 18}$$

For the series expansion in δ^{-1} analogous results hold. Indeed, owing to (15) the maximum absolute values of ξ_k are α^k times the maxima M_k. For the inverse radius of convergence of the series expansion in δ^{-1}, which we denote by μ, we therefore have $\mu = \alpha\rho$, as can be seen readily from (A 18).

To obtain the value of ρ we calculated M_k by searching for the largest absolute value of ζ_k among the points of a rectangular 51×51 grid $x_{ij} = -1+(i-1)/25$, $y_{ij} = -1+(j-1)/25$ for which $x_{ij}^2+y_{ij}^2 \leqslant 1$. As a typical example we show in figure 8 for $\alpha = 1$ the values of $\ln M_k$ as a function of k. The figure strongly suggests that, for large values of k, we have

$$\ln M_k \sim \ln a + k\ln b, \tag{A 19}$$

where $\ln a$ and $\ln b$ are constants, i.e. asymptotically $\ln M_k$ becomes a linear function of k. This means that ρ is given by

$$\rho = \limsup_{k\to\infty} \exp\left(\frac{\ln a + k\ln b}{k}\right) = b. \tag{A 20}$$

The value of b can be determined by applying a least-squares fit of a linear graph through the points with $k = 30$ to 50, giving for $\ln\rho$ the value -1.44. The accuracy of the value thus obtained can be estimated by repeating the fit for several other ranges of k and leads to an estimated accuracy of 1%. The calculation of the inverse radius

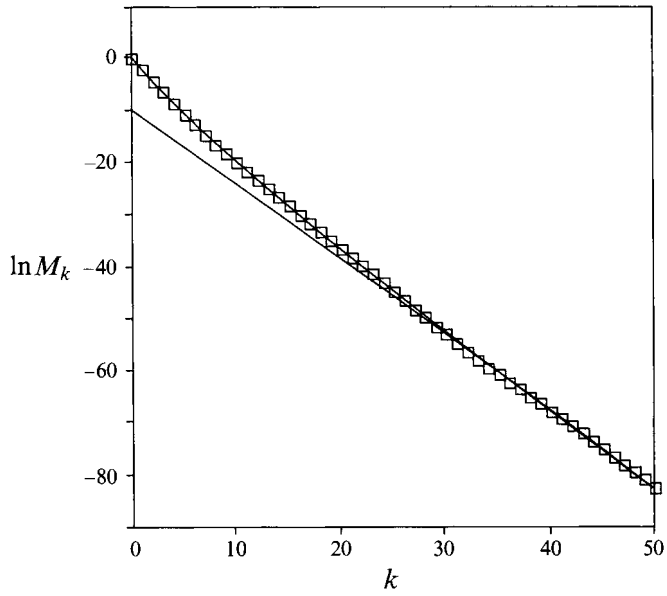

FIGURE 8. Graph of $\ln M_k$ as a function of k (for $\alpha = 1$), where M_k is the maximum absolute value of ζ_k and k is the order of the expansion in κ^{-1}. The value of M_k was obtained numerically by searching for the maximum absolute value of ζ_k within the circular basin on a rectangular 51×51 grid. The graph shows that $\ln M_k$ asymptotes to a linear descending line, the slope of which gives the inverse radius of convergence of the series expansion.

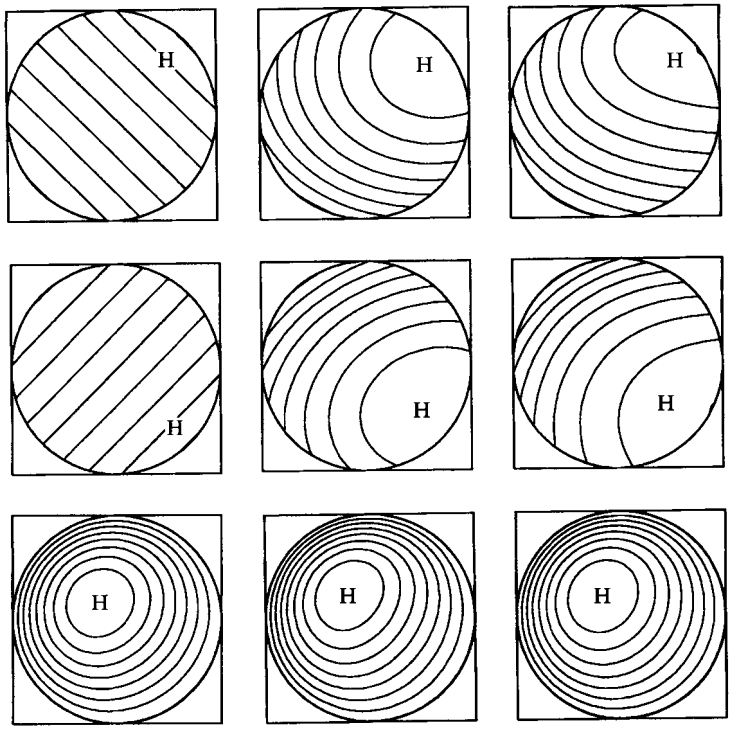

FIGURE 9. The absolute vorticity (upper row), relative vorticity (middle row) and streamfunction (bottom row) of the solution with parameters $(\ln\alpha, \ln\kappa) = (0, -0.75)$ (point A in figure 1) and for different lengths of the expansions in κ^{-1}. In the first column of the figure the terms were summed up to $k = 0$, in the second column up to $k = 1$ and in the third column up to $k = 50$.

of convergence was carried out for a large set of α-values. The results are displayed in figure 1, as explained in §2.3. The solid curve in figure 1 is a graph of $\ln\rho$ as a function of $\ln\alpha$. So, points above this curve correspond to parameters α, κ and δ for which the series expansion for ζ converges uniformly. Points beneath the curve correspond to parameters for which the series expansion does not converge uniformly, although the series might converge locally. For clarity the region beneath the curve has been shaded.

To illustrate the rate of convergence, we consider the absolute vorticity $\zeta+y$, relative vorticity ζ and streamfunction ψ for $(\ln\alpha, \ln\kappa) = (0, -0.75)$ or, equivalently, for $(\ln\alpha, \ln\delta) = (0, -0.75)$ (point A in figure 1) for different lengths of the expansions. So, in the first column of figure 9 the three fields $\zeta+y$, ζ and ψ are summed to order 0, in the second column to order 1 and in the third column to order 50. The figure shows quite clearly that the convergence is rapid. Indeed, even the solution to order 1, of which we have given the analytic expressions in §2, quite adequately gives us an idea of the full solution.

REFERENCES

BEARDSLEY, R. C. 1969 A laboratory model of the wind-driven ocean circulation. *J. Fluid Mech.* **38**, 255–271.

FOFONOFF, N. P. 1954 Steady flow in a frictionless homogeneous ocean. *J. Mar. Res.* **13**, 254–262.

FOFONOFF, N. P. 1962 Dynamics of ocean currents. In *The Sea, vol. 1: Physical Oceanography* (ed. M. N. Hill), pp. 3–30. Interscience.

GREATBATCH, R. J. 1987 A model for the inertial recirculation of a gyre. *J. Mar. Res.* **45**, 601–634.

HARRISON, D. E. & STALOS, J. 1982 On the wind-driven ocean circulation. *J. Mar. Res.* **40**, 773–791.

HØILAND, E. 1950 On horizontal motion in a rotating fluid. *Geofys. Publik.* **17**, 1–26.

HOLLOWAY, G. 1986 Comment on Fofonoff's mode. *Geophys. Astrophys. Fluid Dyn.* **37**, 165–169.

MARSHALL, J. & NURSER, G. 1986 Steady, free circulation in a stratified quasi-geostrophic ocean. *J. Phys. Oceanogr.* **16**, 1799–1813.

MERKINE, L.-O., MO, K. C. & KALNAY, E. 1985 On Fofonoff's mode. *Geophys. Astrophys. Fluid Dyn.* **32**, 175–196.

MILLER, J., WEICHMAN, P. B. & CROSS, M. C. 1992 Statistical mechanics, Euler's equations and Jupiter's red spot. *Phys. Rev.* A **45**, 2328–2359.

NIILER, P. P. 1966 On the theory of wind-driven ocean circulation. *Deep-Sea Res.* **13**, 597–606.

PEDLOSKY, J. 1987 *Geophysical Fluid Dynamics.* Springer.

PIERREHUMBERT, R. T. & MALGUZZI, P. 1984 Forced coherent structures and local multiple equilibria in a barotropic atmosphere. *J. Atmos. Sci.* **41**, 246–257.

ROBERT, R. & SOMMERIA, J. 1991 Statistical equilibrium states for two-dimensional flows. *J. Fluid Mech.* **229**, 291–310.

RUDIN, W. 1964 *Principles of Mathematical Analysis.* McGraw-Hill.

SALMON, R., HOLLOWAY, G. & HENDERSHOTT, M. C. 1976 The equilibrium statistical mechanics of simple quasi-geostrophic models. *J. Fluid Mech.* **75**, 691–703.

STOMMEL, H. 1948 The westward intensification of wind-driven ocean currents. *Trans. Am. Geophys. Union* **99**, 202–206.

SWART, H. E. DE & ZIMMERMAN, J. T. F. 1993 Rectification of the wind-driven ocean circulation on the β plane. *Geophys. Astrophys. Fluid Dyn.* **71**, 17–41.

VERONIS, G. 1966*a* Wind-driven ocean circulation – part I: linear theory and perturbation analysis. *Deep-Sea Res.* **13**, 17–29.

VERONIS, G. 1966*b* Wind-driven ocean circulation – part II: numerical solution of the nonlinear problem. *Deep-Sea Res.* **13**, 31–55.

ZIMMERMAN, J. T. F. 1993 A simple model for the symmetry properties of nonlinear wind-driven ocean circulation. *Geophys. Astrophys. Fluid Dyn.* **71**, 1–15.

ZIMMERMAN, J. T. F. & MAAS, L. R. M. 1989 Renormalized Green's function for nonlinear circulation on the beta plane. *Phys. Rev.* A **39**, 3575–3590.